

## Analysis of a Generic Model of Eukaryotic Cell-Cycle Regulation

Attila Csikász-Nagy,<sup>\*†</sup> Dorjsuren Battogtokh,<sup>\*</sup> Katherine C. Chen,<sup>\*</sup> Béla Novák,<sup>†</sup> and John J. Tyson<sup>\*</sup>

<sup>\*</sup>Department of Biological Sciences, Virginia Polytechnic Institute and State University, Blacksburg, Virginia 24061-0406; and <sup>†</sup>Molecular Network Dynamics Research Group of the Hungarian Academy of Sciences and Department of Agricultural and Chemical Technology, Budapest University of Technology and Economics, H-1521 Budapest, Hungary

**ABSTRACT** We propose a protein interaction network for the regulation of DNA synthesis and mitosis that emphasizes the universality of the regulatory system among eukaryotic cells. The idiosyncrasies of cell cycle regulation in particular organisms can be attributed, we claim, to specific settings of rate constants in the dynamic network of chemical reactions. The values of these rate constants are determined ultimately by the genetic makeup of an organism. To support these claims, we convert the reaction mechanism into a set of governing kinetic equations and provide parameter values (specific to budding yeast, fission yeast, frog eggs, and mammalian cells) that account for many curious features of cell cycle regulation in these organisms. Using one-parameter bifurcation diagrams, we show how overall cell growth drives progression through the cell cycle, how cell-size homeostasis can be achieved by two different strategies, and how mutations remodel bifurcation diagrams and create unusual cell-division phenotypes. The relation between gene dosage and phenotype can be summarized compactly in two-parameter bifurcation diagrams. Our approach provides a theoretical framework in which to understand both the universality and particularity of cell cycle regulation, and to construct, in modular fashion, increasingly complex models of the networks controlling cell growth and division.

### INTRODUCTION

The cell cycle is the sequence of events by which a cell replicates its genome and distributes the copies evenly to two daughter cells. In most cells, the DNA replication-division cycle is coupled to the duplication of all other components of the cell (ribosomes, membranes, metabolic machinery, etc.), so that the interdivision time of the cell is identical to its mass doubling time (1,2). Usually mass doubling is the slower process; hence, temporal gaps (G1 and G2) are inserted in the cell cycle between S phase (DNA synthesis) and M phase (mitosis). During G1 and G2 phases, the cell is growing and “preparing” for the next major event of the DNA cycle (3). “Surveillance mechanisms” monitor progress through the cell cycle and stop the cell at crucial “checkpoints” so that events of the DNA and growth cycles do not get out of order or out of balance (4,5). In particular, in protists (for sure) and metazoans (to a lesser extent), cells must grow to a critical size to start S phase and to a larger size to enter mitosis. These checkpoint requirements assure that the cycle of DNA synthesis and mitosis will keep pace with the overall growth of cells (6). Other checkpoint signals monitor DNA damage and repair, completion of DNA replication, and congression of replicated chromosomes to the metaphase plate (7).

### Eukaryotic cell cycle engine

These interdependent processes are choreographed by a complex network of interacting genes and proteins. The main

components of this network are cyclin-dependent protein kinases (Cdk's), which initiate crucial events of the cell cycle by phosphorylating specific protein targets. Cdk's are active only if bound to a cyclin partner. Yeasts have only one essential Cdk, which can induce both S and M phase depending on which type of cyclin it binds. Because Cdk molecules are always present in excess, it is the availability of cyclins that determines the number of Cdk/cyclin complexes in a cell (8). Cdk/cyclin complexes can be down-regulated a), by inhibitory phosphorylation of the Cdk subunit and b), by binding to a stoichiometric inhibitor (cyclin-dependent kinase inhibitor (CKI)) (9).

Some years ago Paul Nurse (10) proposed, and since then many experimental studies have confirmed, that the DNA replication-division cycle in all eukaryotic cells is controlled by a common set of proteins interacting with each other by a common set of rules. Nonetheless, each particular organism seems to use its own peculiar mix of these proteins and interactions, generating its own idiosyncrasies of cell growth and division. The “generic” features of cell cycle control concern these common genes and proteins and the general dynamical principles by which they orchestrate the replication and partitioning of the genome from mother cell to daughter. The peculiarities of the cell cycle concern exactly which parts of the common machinery are functioning in any given cell type, given the genetic background and developmental stage of an organism. We formulate the genericity of cell cycle regulation in terms of an “underlying” set of nonlinear ordinary differential equations with unspecified kinetic parameters, and we attribute the peculiarities of specific organisms to the precise settings of these parameters. Using bifurcation diagrams, we show how specific physiological features of

*Submitted January 12, 2006, and accepted for publication March 16, 2006.*

Address reprint requests to John J. Tyson, Tel.: 540-231-4662; Fax: 540-231-9307; E-mail: tyson@vt.edu; or Attila Csikász-Nagy, E-mail: csikasz@mail.bme.hu.

© 2006 by the Biophysical Society

0006-3495/06/06/4361/19 \$2.00

doi: 10.1529/biophysj.106.081240

the cell cycle are determined ultimately by levels of gene expression.

### Mathematical modeling of the cell cycle

The dynamic properties of complex regulatory networks cannot be reliably characterized by intuitive reasoning alone. Computers can help us to understand and predict the behavior of such networks, and differential equations (DEs) provide a convenient language for expressing the meaning of a molecular wiring diagram in computer-readable form (11). Numerical solutions of the DEs can be compared with experimental results, in an effort to determine the kinetic rate constants in the model and to confirm the adequacy of the wiring diagram. Eventually the model, with correct equations and rate constants, should give accurate simulations of known experimental results and should be pressed to make verifiable predictions. This method has been used for many years to create mathematical models of eukaryotic cell cycle regulation (12–29). The greatest drawback to DE-based modeling is that the modeler must estimate all the rate constants from the available data and still have some observations “left over” to test the model. In the case of cell cycle regulation, very few of these rate constants have been measured directly (30,31) although the available data provide severe constraints on rate constant values (15,32). To complement the important but tedious work of parameter estimation by data fitting, we need analytical tools for

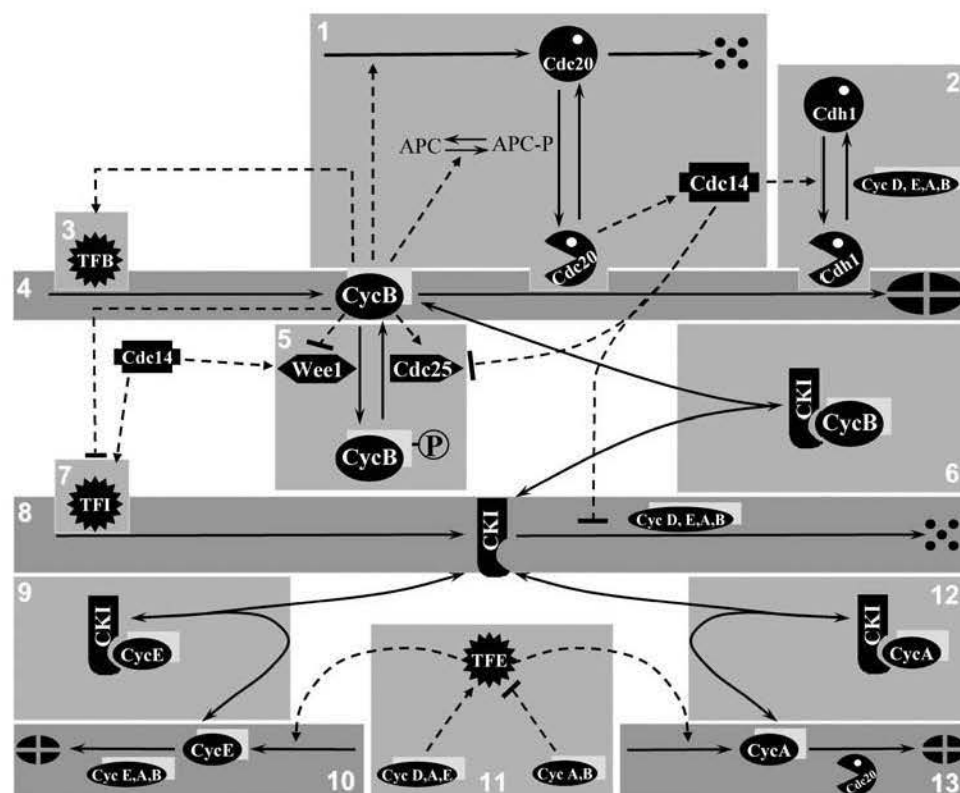
characterizing the parameter-dependence of solutions of DEs and for associating a model’s robust dynamical properties to the physiological characteristics of living cells.

### Bifurcation theory and regulatory networks

Bifurcation theory is a general tool for classifying the attractors of a dynamical system and describing how the qualitative properties of these attractors change as a parameter value changes. Bifurcation theory has been used successfully to understand transitions in the cell cycle by our group (33–37) and by others (12,26,38). In this article, we use bifurcation theory to examine a generic model of eukaryotic cell cycle controls, bringing out the similarities and differences in the dynamical regulation of cell cycle events in yeasts, frog eggs, and mammalian cells. To understand our approach, the reader must be familiar with a few elementary bifurcations of nonlinear DEs and how they are generated by positive and negative feedback in the underlying molecular network. For more details, the reader may consult the Appendix to this article and some recent review articles (36,37).

### MATERIALS AND METHODS

In Fig. 1 we propose a general protein interaction network for regulating cyclin-dependent kinase activities in eukaryotic cells. (Fig. 1 uses “generic” names for each protein; in Table 1 we present the common names of each component in specific cell types: budding yeast, fission yeast, frog eggs, and



**FIGURE 1** Wiring diagram of the generic cell-cycle regulatory network. Chemical reactions (solid lines), regulatory effects (dashed lines); a protein sitting on a reaction arrow represents an enzyme catalyst of the reaction. Regulatory modules of the system are distinguished by shaded backgrounds: (1) exit of M module, (2) Cdh1 module, (3) CycB transcription factor, (4) CycB synthesis/degradation, (5) G2 module, (6) CycB inhibition by CKI (also includes the binding of phosphorylated CycB, if that is present), (7) CKI transcription factor, (8) CKI synthesis/degradation, (9) CycE inhibition by CKI, (10) CycE synthesis/degradation, (11) CycE/A transcription factor, (12) CycA inhibition by CKI, (13) CycA synthesis/degradation. Open-mouthed PacMan represents active form of regulated protein; gray rectangles behind cyclins represent their Cdk partners. We assume that all Cdk subunits are present in constant, excess amounts.

**TABLE 1** Protein name conversion table and modules used for each organism

In Fig. 1	Budding yeast	Fission yeast	<i>Xenopus</i> embryo	Mammalian cells	Function
CycB	Cdc28/Cib1,2	Cdc2/Cdc13	Cdc2/CycB	Cdc2/CycB	Mitotic Cdk/cyclin complex
CycA	Cdc28/Cib5,6	Cdc2/Cig2	Cdk1,2/CycA	Cdk1,2/CycA	S-phase Cdk/cyclin complex
CycE	Cdc28/Cln1,2	—	Cdk2/CycE	Cdk2/CycE	G1/S transition inducer Cdk/cyclin
CycD	Cdc28/Cln3	Cdc2/Puc1	Cdk4,6/CycD	Cdk4,6/CycD	Starter Cdk/cyclin complex
CKI	Sic1	Rum1	Xic1	p27 <sup>Kip1</sup>	Cdk/cyclin stoichiometric inhibitor
Cdh1	Cdh1	Ste9	Fzr	hCdh1	CycB degradation regulator with APC
Wee1	Swe1	Wee1	Xwee1	hWee1	Cdk/CycB inhibitory kinase
Cdc25	Mih1	Cdc25	Xcdc25	Cdc25C	Cdk/CycB activatory phosphatase
Cdc20	Cdc20	Slp1	Fizzy	p55 <sup>Cdc</sup>	CycB, CycA degradation regulator with APC
Cdc14	Cdc14	Clp1/Flp1	Xcdc14	hCdc14	Phosphatase working against the Cdk's
TFB	Mcm1	—	—	Mcm	CycB transcription factor
TFE	Swi4/Swi6 Mbp1/Swi6	Cdc10/Res1	XE2F	E2F	CycE/A transcription factor (SBF+MBF in budding yeast)
TFI	Swi5	—	—	—	CKI transcription factor
APC	APC	APC	APC	APC	Anaphase promoting complex
Active modules	1, 2, 3, 4, 6, 7, 8, 10, 11, 12, 13, (5*)	1, 2, 4, 5, 6, 8, 11, 12, 13	1, 4, 5	1, 2, 3, 4, 6, 8, 9, 10, 11, 12, 13, (5*)	Modules of Fig. 1, used for simulation of organism

\*Module 5 is not introduced into the first version of budding yeast and mammalian models.

mammalian cells.) Using basic principles of biochemical kinetics, we translate the generic mechanism into a set of coupled nonlinear ordinary differential equations (Supplementary Material, Table SI) for the temporal dynamics of each protein species. Although the structure of the DEs is fixed by the topology of the network, the forms of the reaction rate laws (mass action, Michaelis-Menten, etc.) are somewhat arbitrary and would vary from one modeller to another. We use rate laws consistent as much as possible with our earlier choices (15,18,25,39–41). In addition, most of the parameter values for each organism (Supplementary Material, Table SII) were inherited from earlier models.

For numerical simulations and bifurcation analysis of the DEs, we used the computer program XPP-AUT (42), with the “stiff” integrator. Instructions on how to reproduce our simulations and diagrams (including all necessary .ode and .set files, and an optional SBML version of the model) can be downloaded from our website (43).

All protein concentrations in the model are expressed in arbitrary units (au) because, for the most part, we do not know the actual concentrations of most regulatory proteins in the cell. Hence, all rate constants capture only the timescales of processes (rate constant units are  $\text{min}^{-1}$ ). For each mutant, we use the same equations and parameter values except for those rate constants that are changed by the mutation (e.g., for gene deletion we set the synthesis rate of the associated protein to zero).

## RESULTS

### A generic model of cell cycle regulation

Since the advent of gene-cloning technologies in the 1980s, molecular cell biologists have been astoundingly successful in unraveling the complex networks of genes and proteins that underlie major aspects of cell physiology. These results have been collected recently in comprehensive molecular interaction maps (44–48). In the same spirit, but with an eye toward a computable, dynamic model, we collected the most important regulatory “modules” of the Cdk network. Our goal is to describe a generic network (Fig. 1) that applies equally well to yeasts, frogs, and humans. We do not claim that Fig. 1 is a complete model of eukaryotic cell-cycle con-

trols, only that it is a starting point for understanding the basic cell-cycle engine across species.

### Regulatory modules

The network, which tracks the three principal cyclin families (cyclins A, B, and E) and the proteins that regulate them at the G1-S, G2-M, and M-G1 transitions, can be subdivided into 13 modules. (Other, coarser subdivisions are possible, but these 13 modules are convenient for describing the similarities and differences of regulatory signals among various organisms.)

Modules 4, 10, and 13: synthesis and degradation of cyclins B, E, and A. Cyclin E is active primarily at the G1-S transition, cyclin A is active from S phase to early M phase, and cyclin B is essential for mitosis.

Modules 1 and 2: regulation of the anaphase promoting complex (APC). The APC works in conjunction with Cdc20 and Cdh1 to ubiquitinyrate cyclin B, thereby labeling it for degradation by proteasomes. The APC must be phosphorylated by the mitotic CycB kinase before it will associate readily with Cdc20, but not so with Cdh1. On the other hand, Cdh1 can be inactivated by phosphorylation by cyclin-dependent kinases. Cdc14 is a phosphatase that opposes Cdk by dephosphorylating and activating Cdh1.

Module 8: synthesis and degradation of CKI (cyclin-dependent kinase inhibitor). Degradation of CKI is promoted by phosphorylation by cyclin-dependent kinases and inhibited by Cdc14 phosphatase.

Modules 6, 9, and 12: reversible binding of CKI to cyclin/Cdk dimers to produce catalytically inactive trimers (stoichiometric inhibition).

Modules 3, 7, and 11: regulation of the transcription factors that drive expression of cyclins and CKI. TFB is activated by cyclin B-dependent kinase. TFE is activated by some cyclin-dependent kinases and inhibited by others. TFI

is inhibited by cyclin B-dependent kinase and activated by Cdc14 phosphatase.

Module 5: regulation of cyclin B-dependent kinase by tyrosine phosphorylation and dephosphorylation (by Wee1 kinase and Cdc25 phosphatase, respectively). The tyrosine-phosphorylated form is less active than the unphosphorylated form. Cyclin B-dependent kinase phosphorylates both Wee1 (inactivating it) and Cdc25 (activating it), and these phosphorylations are reversed by Cdc14 phosphatase.

The model is replete with positive feedback loops (CycB activates TFB, which drives synthesis of CycB; CycB activates Cdc25, which activates CycB; CKI inhibits CycB, which promotes degradation of CKI; Cdh1 degrades CycB, which inhibits Cdh1), and negative feedback loops (CycB activates APC, which activates Cdc20, which degrades CycB; CycB activates Cdc20, which activates Cdc14, which opposes CycB; TFE drives synthesis of CycA, which inhibits TFE). These complex, interwoven feedback loops create the interesting dynamical properties of the control system, which account for the characteristic features of cell cycle regulation, as we intend to show.

The model (at present) neglects important pathways that regulate, e.g., cell proliferation in metazoans (retinoblastoma protein), mitotic exit in yeasts (the FEAR, MEN, and SIN pathways), and the ubiquitous DNA-damage and spindle assembly checkpoints. We intend to remedy these deficiencies in later publications, as we systematically grow the model to include more and more features of the control system.

#### *Role of cell growth*

In yeasts and other lower eukaryotes, a great deal of evidence shows the dominant role of cell growth in setting the tempo of cell division (2,49–52). In somatic cells of higher eukaryotes there are many reports of size control of cell-cycle events (e.g., (53–55)), although other authors have cast doubts on a regulatory role for cell size (e.g., (56,57)). For embryonic cells and cell extracts, the activation of Cdk1 is clearly dependent on the total amount of cyclin B available (58,59). To create a role for cell size in the regulation of Cdk activities, we assume, in our models, that the rates of synthesis of cyclins A, B, and E are proportional to cell “mass”. The idea behind this assumption (see also Futcher (60)) is that cyclins are synthesized in the cytoplasm on ribosomes at an increasing rate as the cell grows. The cyclins then find a Cdk partner and move into the nucleus where they perform their functions. Presumably the effective, intranuclear concentrations of the cyclin-dependent kinases increase as the cell grows because they become more concentrated at their sites of action. Other regulatory proteins in the network, we assume, are not compartmentalized in the same way, so their effective concentrations do not increase as the cell grows. This basic idea for size control of the cell cycle was tested experimentally in budding yeast by manipulating the “nuclear localization signals” on cyclin proteins (8). As pre-

dicted by the model, cell size is larger in cells that exclude cyclins from the nucleus and smaller in cells that overaccumulate cyclins in the nucleus. A recent theoretical study by Yang et al. (61) may shed light on how cell size couples to cell division without assuming a direct dependence of cyclin synthesis rate on mass, but, for this article, we adopt the assumption as a simple and effective way to incorporate size control into nonlinear DE models for the control of cyclin-dependent kinase activities.

For simplicity, we assume that cell mass increases exponentially (with a mass doubling time (MDT) suitable for the organism under consideration) and that cell mass is exactly halved at division. Our qualitative results (bifurcation diagrams, etc.) are not dependent on these assumptions. Cell growth may be linear or logistic, and cell division may be asymmetric or inexact—it doesn’t really matter to our models. The important features are that “mass” increases monotonically as the cell grows (driving the control system through bifurcations that govern events of the cell cycle) and that mass decreases abruptly at cell division (resetting the control system back to a G1-like state—unreplicated chromosomes and low Cdk activity).

#### *Equations and parameter values*

The dynamical properties of the regulatory network in Fig. 1 can be described by a set of ordinary differential equations (Supplementary Material, Table SI), given a table of parameter values suitable for specific organisms (Table SII). For each organism we analyze the effects of physiological and genetic changes on the transitions between cell cycle phases, in terms of bifurcations of the vector fields defined by the DEs (for background on dynamical systems, see the Appendix).

#### **Frog embryos: *Xenopus laevis***

To validate our equations and tools, we first verified our earliest studies of bifurcations in the frog-egg model. The combination of modules 1, 4, and 5 of Fig. 1 was used to recreate the bifurcation diagram of Borisuk and Tyson (33); see Supplementary Material, Fig. S1. Our bifurcation parameter, “cell mass”, can be interpreted as the rate constant for cyclin B synthesis. For small rates of cyclin synthesis, the control system is arrested in a stable “interphase” state with low activity of CycB-dependent kinase. For larger rates of cyclin synthesis, the model exhibits spontaneous limit cycle oscillations, which begin at a SNIPER bifurcation (long period, fixed amplitude). Eventually, as the rate of cyclin synthesis gets large enough, the oscillations are lost at a Hopf bifurcation (fixed period, vanishing amplitude). Beyond the Hopf bifurcation, the control system is arrested in a stable “mitotic” state with high activity of CycB-dependent kinase. These types of states of the control system are reminiscent of the three characteristic states of frog eggs: interphase arrest (immature oocyte), metaphase arrest (mature oocyte), and



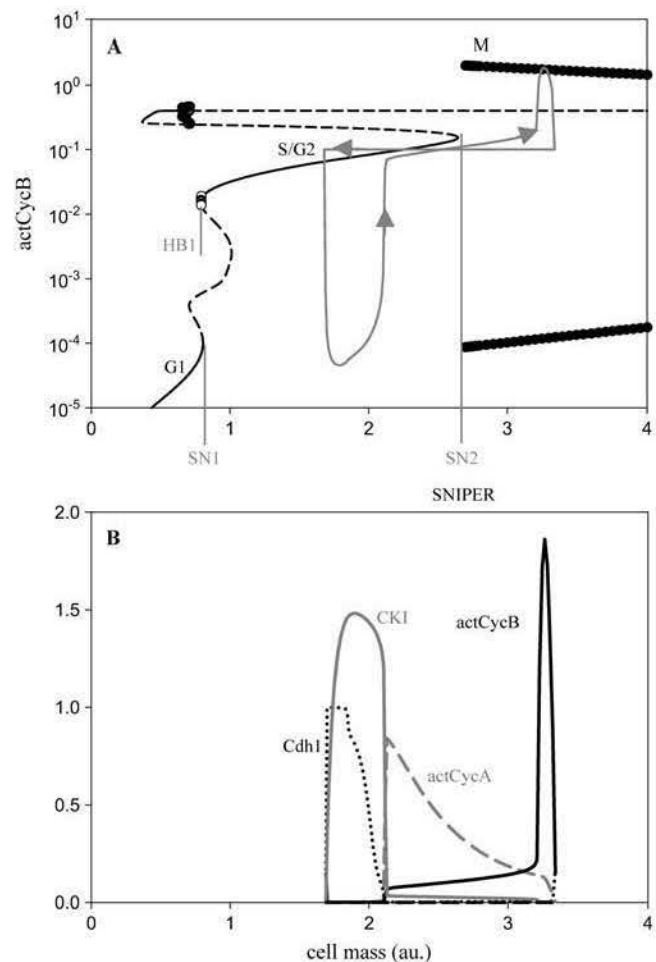
spontaneous oscillations (fertilized egg). For more details, see Novak and Tyson (18) and Borisuk and Tyson (33).

### Fission yeast: *Schizosaccharomyces pombe*

#### Wild-type cell cycle

The fission yeast cell cycle network, composed of modules 1, 2, 4, 5, 6, 8, 11, 12, and 13, is described in Fig. 2 in terms of a one-parameter bifurcation diagram (Fig. 2A) and a simulation (Fig. 2B). In the simulation, we plot protein levels as a function of cell mass rather than time, but because mass increases exponentially with time, one may think of the lower abscissa as  $e^{\mu t}$ . We present the simulation this way so that we can “lift it up” onto the bifurcation diagram: the gray curve in Fig. 2A is identical to the solid black curve (actCycB) in Fig. 2B. In Fig. 2A, a stable, G1-like, steady state exists at very low level of actCycB (active Cdk/CycB dimers). This steady state is lost at a saddle-node bifurcation (SN1) at cell mass = 0.8 au. Between SN1 and SN2 (at cell mass = 2.6 au), the control system has a single, stable, steady-state attractor with an intermediate activity ( $\sim 0.1$ ) of cyclin B (an S/G2-like steady state). The other steady-state branches are unstable and physiologically unnoticeable. For mass  $>2.6$  au, the only stable attractor is a stable limit cycle oscillation. This branch of stable limit cycles is lost by further bifurcations at very large mass (of little physiological significance for wild-type cells).

The gray trajectory in Fig. 2A represents the path of a growing-dividing yeast cell projected onto the bifurcation diagram. Let us pick up the trajectory of a growing cell at mass = 2.2 au, where the cell cycle control system has been captured by the stable S/G2 steady state. As the cell continues to grow, it leaves the S/G2 state at SN2 and prepares to enter mitosis. At cell mass  $>2.6$ , the only stable attractor is a limit cycle. This limit cycle, which bifurcates from SN2, has infinite period at the onset of the bifurcation (hence, the onset point is commonly called a SNIPER—saddle-node-infinite-period—bifurcation). Because the limit cycle has a very long period at first, and the cell enters the limit cycle at the place where the saddle-node used to be, the cell is stuck in a semistable transient state (where the gray trajectory “overshoots” SN2). As the cell grows, it eventually escapes the semistable state (at cell mass  $\approx 3$ ), and then actCycB increases dramatically (note the log-scale on the ordinate), driving the cell into mitosis. Because the control system is now captured by the stable limit cycle, actCycB inevitably decreases and the cell is driven out of mitosis. We presume that the cell divides when actCycB falls below 0.1; hence, cell mass is halved ( $3.4 \rightarrow 1.7$ ), and the control system is now attracted to the S/G2 steady state (the only stable attractor at this cell mass). The newly divided cell makes its way to the S/G2 attractor by a circuitous route that looks like a brief G1 state (very low actCycB) but is not a stable and long-lasting G1 state. This transient G1 state is characteristic of wild-type fission yeast cells (62).



**FIGURE 2** One-parameter bifurcation diagram (A) and cell-cycle trajectory (B) of wild-type fission yeast. Both figures share the same abscissa. Notice that cell mass is just the logarithm of age, because we assume that cells grow exponentially between birth (age = 0) and division (age = MDT). The gray curve in panel A (a “cell-cycle trajectory” for MDT = 120 min) is identical to the solid black curve in panel B. Key to panel A: solid line, stable steady state; dashed line, unstable steady state; solid circles, maxima and minima of stable oscillations; open circles, maxima and minima of unstable oscillations; SN1 (saddle-node bifurcation that annihilates the G1 steady state), SN2 (saddle-node bifurcation that annihilates the G2 steady state), and HB1 (Hopf bifurcation on the S/G2 branch of steady states that gives rise to endoreplication cycles). SN2 is a SNIPER bifurcation; i.e., it gives way to stable periodic solutions of infinite period (at the bifurcation point). The other (unmarked) bifurcation points in this diagram are not pertinent to cell-cycle regulation.

Overshoot of a SNIPER bifurcation point (as in Fig. 2A) is a common feature of our cell cycle models, and recent experimental evidence (63) confirms this prediction in frog egg extracts. These authors located the position of the steady-state SN bifurcation in a nonoscillatory extract and then showed that during oscillations the Cdk-regulatory system overshoots the SN point by twofold or more.

The one-parameter bifurcation diagram in Fig. 2A is a compact way to display the interplay between the DNA replication-segregation cycle (regulated by Cdk/CycB activity)

and the growth-division cycle (represented on the abscissa by the steady increase of cell mass and its abrupt resetting at division). The very strong “cell size control” in late G2 phase of the fission yeast cell cycle, which has been known to physiologists for 30 years (52), is here represented by growing past the SNIPER bifurcation, which eliminates the stable S/G2 steady state and allows the cell to pass into and out of mitosis (the stable limit cycle oscillation).

A satisfactory model of fission yeast must account not only for the phenotype of wild-type cells but also for the unusual properties of the classic *cdc* and *wee* mutants that played such important roles in deducing the cell-cycle control network. Mutations change the values of specific rate constants, which remodel the one-parameter bifurcation diagram and thereby change the way a cell progresses through the DNA replication-division cycle. For example (Fig. 3 A), for a *wee1*<sup>−</sup> mutant (reduce Wee1 activity to 10% of its wild-type value) SN2 moves to the left of SN1 and the infinite-period limit cycle now bifurcates from SN1. Hence, the cell cycle in *wee1*<sup>−</sup> cells is now organized by a SNIPER

bifurcation at the G1/S transition: *wee1*<sup>−</sup> cells are about half the size of wild-type cells, they have a long G1 phase and short G2, and slowly growing cells pause in G1 (unreplicated DNA) rather than in G2 (replicated DNA).

In the Supplementary Material (Fig. S2) we present bifurcation diagrams for four other fission yeast mutants (*cig2*Δ, *cig2*Δ *run1*Δ, *wee1*Δ *cdc25*Δ, *wee1*Δ *run1*Δ), to confirm that our “generic” version is indeed consistent with the known physiology of these mutants. Because they have been described in detail elsewhere (37), we turn our attention instead to some novel results.

#### Endoreplicating mutants

On the wild-type bifurcation diagram (Fig. 2 A) we can notice a very small oscillatory regime at the beginning of the S/G2 branch of steady states (labeled as HB1, at cell mass = 0.79). This stable periodic solution is a consequence of a negative feedback loop whereby Cig2 inhibits its own transcription factor, Cdc10, by phosphorylation (64). (In the generic

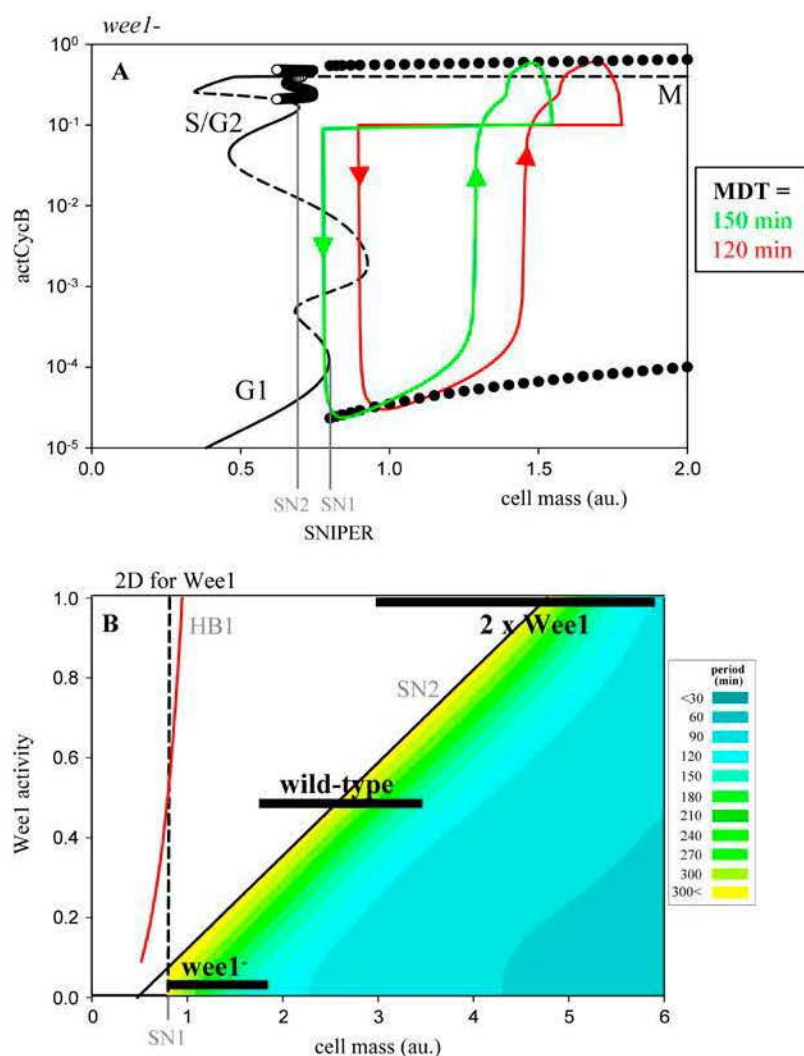


FIGURE 3 One-parameter (A) and two-parameter (B) bifurcation diagrams for mutations at the *wee1* locus in fission yeast. Panel A should be interpreted as in Fig. 2. Key to panel B: dashed black line, locus of SN1 bifurcation points; solid black line, locus of SN2 bifurcation points; red line, locus of HB1 bifurcation points; black bars, projections of the cell-cycle trajectories in Figs. 2 A and 3 A onto the two-parameter plane. Within regions of stable limit cycles, the color code denotes the period of oscillations. Notice that the period becomes very long as the limit cycles approach the locus of SNIPER bifurcations. The limit cycles switch their allegiance from SN2 to SN1 at Wee1 activity  $\sim 0.07$  (by a complex sequence of codimension-two bifurcations that are not indicated here). Notice that *wee1*<sup>+</sup> overexpression leads to large cells, size-controlled at the G2-to-M transition, but *wee1* deletion leads to small cells (half the size of wild-type), size-controlled at the G1-to-S transition.



nomenclature, Cig2 is “CycA” and Cdc10 is “TFE”.) The negative feedback loop can generate oscillations if there is positive feedback in the system as well, which is provided by the Cdk inhibitor (CKI). As CycA slowly accumulates, it is at first sequestered in inactive complexes with CKI, but eventually CycA saturates CKI and active (uninhibited) Cdk/CycA appears. ActCycA phosphorylates CKI, which labels CKI for proteolysis (65). As CKI is degraded, actCycA rises even faster because it is released from the inactive complexes. At this point the negative feedback turns on and CycA synthesis is blocked. With no synthesis but continued degradation, CycA level drops, which allows CKI to come back (provided there is no other Cdk activity that can phosphorylate CKI and keep its level low). CKI comeback returns the control system to G1. In wild-type cells, the CycA-TFE-CKI interactions cannot create stable oscillations because CycB takes over from CycA and keeps CKI low in G2 and M phases. But if CycB is absent (as in *cdc13*Δ mutants of fission yeast), then CKI and CycA generate multiple rounds of DNA replication without intervening mitoses (called “endor-

eplication”), precisely the phenotype of *cdc13*Δ mutants (66).

In Fig. 4 A we show the bifurcation diagram of *cdc13*Δ cells. Over a broad range of cell mass, large amplitude stable oscillations of Cdk/CycA (from a SNIPER bifurcation at SN1) drive multiple rounds of DNA synthesis without intervening mitoses. Because this negative feedback loop also exists in metazoans, it may explain the core mechanism of developmental endoreplication (67).

#### Mutant analysis on the genetics-physiology plane

In our view, genetic mutations are connected to cell phenotypes through bifurcation diagrams. Mutations induce changes in parameter values, which may change the nature of the bifurcations experienced by the control system, which will have observable consequences in the cell's physiology. Mutation-induced changes in parameter values may be large or small: e.g., the rate constant for CycB synthesis = 0 in a *cdc13*Δ cell, but a *wee1*<sup>ts</sup> (“temperature sensitive”) mutant

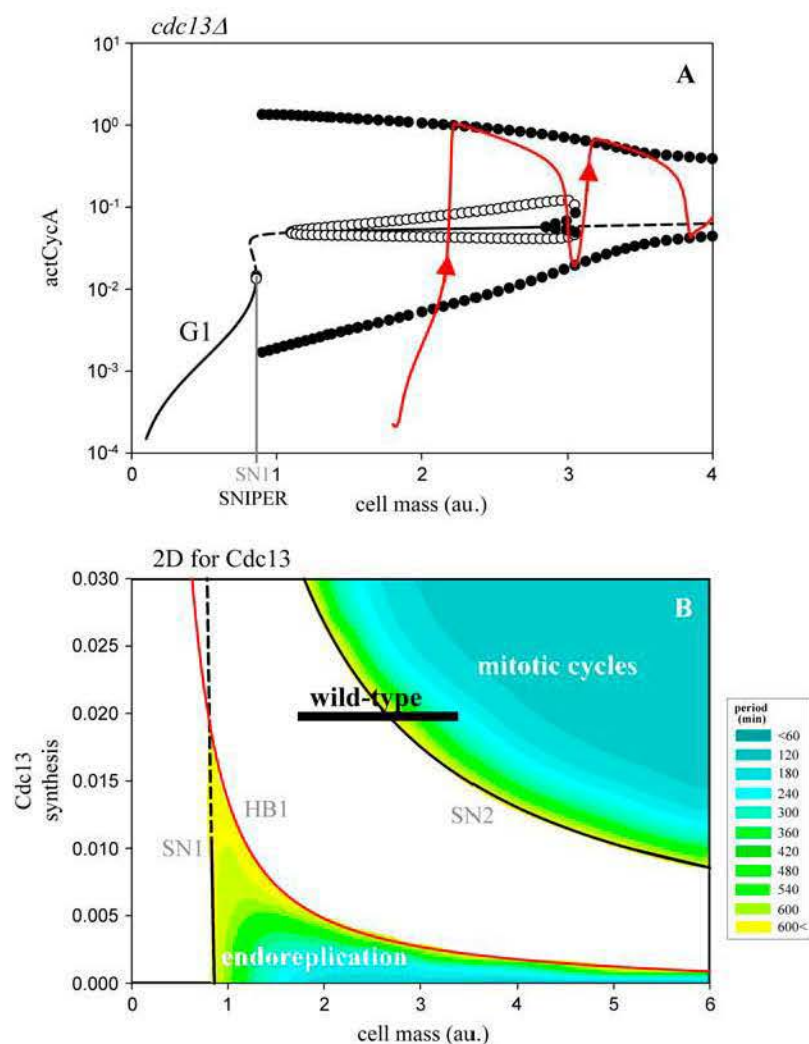


FIGURE 4 One-parameter (A) and two-parameter (B) bifurcation diagrams for mutations at the *cdc13* locus in fission yeast. Panels A and B should be interpreted as in Fig. 3. *cdc13*<sup>+</sup> overexpression has little effect on cell-cycle phenotype, but *cdc13* deletion prevents mitosis and permits endoreplication.

may cause only a minor change in the catalytic activity of Wee1 kinase. Whether these changed parameter values cause a qualitative change in bifurcation points on the one-parameter diagram (Figs. 2 A and 3 A), or merely a quantitative shift of their locations, depends on whether the parameter change crosses a bifurcation point or not. In principle, we can imagine a sequence of bifurcation diagrams (and associated phenotypes) connecting the wild-type cell to a mutant cell as the relevant kinetic parameter changes continuously (up or down) from its wild-type value. This theoretical sequence of morphing phenotypes can be captured on a two-parameter bifurcation diagram, where cell mass continues to stand in for the physiology of the cell cycle (growth and division) and the second parameter is a rate constant that varies continuously between 0 (the deletion mutant) and some large value (the overexpression mutant). Plotted this way, the two-parameter bifurcation diagram spans the entire range of molecular biology from genetics to cell physiology! (For more details on two-parameter bifurcation diagrams, see the Appendix.)

To illustrate this idea, we first consider *wee1* mutations. On the two-parameter bifurcation diagram in Fig. 3 B we follow the loci of bifurcation points (SN1, SN2, and HB1) from their position in wild-type cells (“Wee1 activity” = 0.5) in the direction of overexpression ( $>0.5$ ) or deleterious mutation ( $<0.5$ ). The one-parameter bifurcation diagrams of wild-type (Fig. 2 A) and *wee1*<sup>−</sup> (Fig. 3 A) cells are cuts of this plane at the marked levels of Wee1 activity. For overexpression mutations, the SNIPER bifurcation moves toward larger cell mass, and the heavy bar shows where the simulation of  $2 \times \text{wee1}^+$  cells projects onto the genetics-physiology plane. Clearly, the size of *wee1*<sup>op</sup> cells increases in direct proportion to gene dosage (68). As Wee1 activity decreases below 0.5, e.g., in a heterozygote diploid cell (activity = 0.25) or in *wee1*<sup>ts</sup> mutants, the SNIPER bifurcation moves toward smaller cell mass. Eventually, the SN1 and SN2 loci cross, and the infinite-period oscillations switch from SN2 to SN1 by a short but complicated sequence of codimension-two bifurcations (not shown on the diagram). Because SN1 is not dependent on Wee1 activity, the critical cell size at the SNIPER bifurcation drops no further as Wee1 activity decreases.

The two-parameter bifurcation diagram for cyclin B (Cdc13) expression (Fig. 4 B) shows how mitotic cycles are related to endoreplication cycles. As Cdc13 synthesis rate decreases from its wild-type value ( $0.02 \text{ min}^{-1}$ ), there is a dramatic increase of the critical cell mass for mitotic oscillations (the SNIPER bifurcation associated with SN2). In addition, endoreplication cycles appear at the intersection of HB1 and SN1 (by a sequence of codimension-two bifurcations, which we are not focusing on here). At first appearance, the endoreplication cycles have a very long period, but as Cdc13 synthesis rate decreases further, the period of endoreplication cycles decreases and the range of these oscillations increases.

The two-parameter bifurcation diagrams in Figs. 3 and 4 are incomplete: they do not show all loci of codimension-one bifurcations or any of the characteristic codimension-two bifurcations. Examples of more complete two-parameter bifurcation diagrams can be found in the Supplementary Material (Fig. S3) and on our web site (69).

### Budding yeast: *Saccharomyces cerevisiae*

Our generic model of the budding yeast cell cycle is based on a detailed model published recently by Chen et al. (15). The generic model bypasses details of the mitotic exit network (MEN) in Chen’s model, assuming instead that Cdc20 directly activates Cdc14. We had to change some parameters compared to Chen et al. (15) because of this and other minor changes in the network. We found these new parameter values by fitting simulations of wild-type and some mutant cells (15).

#### Wild-type cells

One-dimensional bifurcation diagrams of wild-type cells created by the full model (15) and by our generic model (Fig. 5, A and B) look very similar. Both figures show a stable G1 steady state that disappears at a SNIPER bifurcation (G1-S transition at cell mass = 1.13 au), giving rise to oscillations that correspond to progression through S/G2/M phases. There is no attractor representing a stable G2 phase in wild-type budding yeast cells. The green, red, and blue curves superimposed on the bifurcation diagram are “cell cycle trajectories” at mass doubling time of 150, 120, and 90 min, respectively ( $\text{MDT} = \ln 2 / \mu$ , where  $\mu$  = specific growth rate). Notice that cells get larger as MDT gets smaller (as  $\mu$  increases). For simplicity, we are neglecting the asymmetry of division of budding yeast in these simulations.

#### Two ways to achieve size homeostasis

Fig. 5 A shows that the relation of the cell cycle trajectory to the SNIPER bifurcation point depends strongly on MDT. At slow growth rates ( $\text{MDT} \geq 150 \text{ min}$ ), newborn cells are smaller than the size at the SNIPER bifurcation; hence the Cdk-control system is attracted to the stable G1 steady state (seen more clearly in Fig. 5 B than in Fig. 5 A), and the cell is waiting until it grows large enough to surpass the SNIPER bifurcation. Only then can the cell commit to the S/G2/M sequence. This is a mathematical representation of the classic notion of “size control” to achieve balanced cell growth and division (49,50,52,70). At faster growth rates, however, newborn cells are already larger than the critical size at the SNIPER bifurcation, and they do not linger in a stable G1 state, waiting to grow large enough to start the next chromosome replication cycle. How then is cell-size homeostasis achieved, if the classic “sizer” mechanism is inoperative?



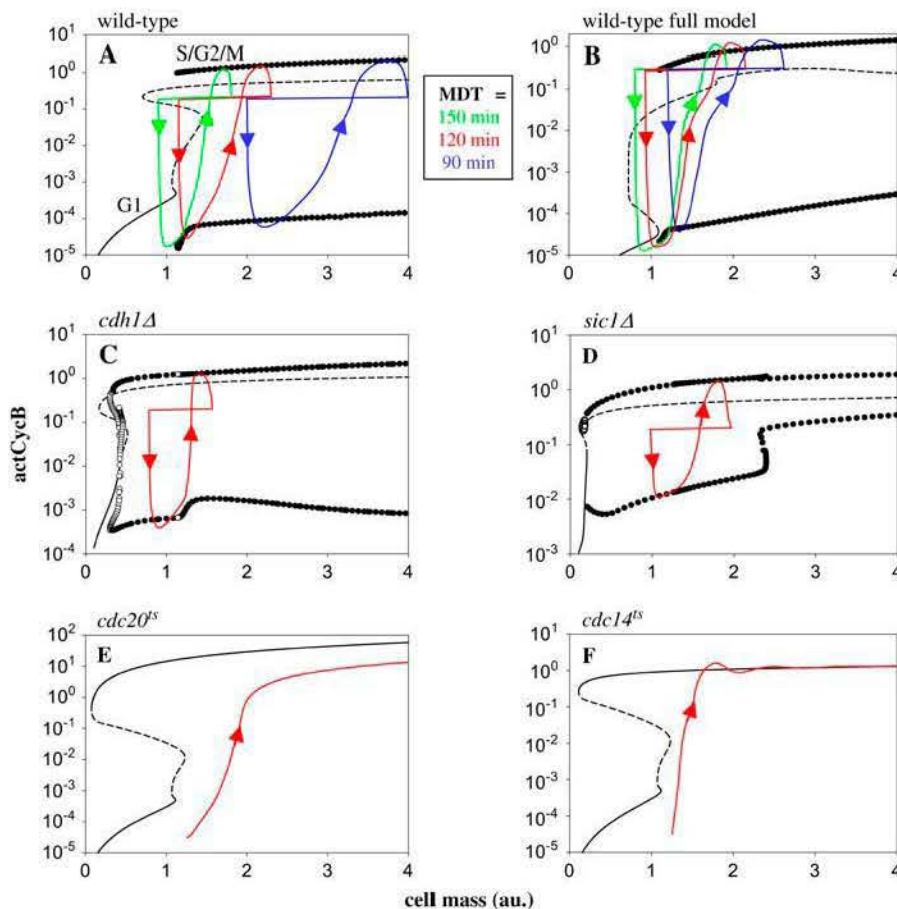


FIGURE 5 One-parameter bifurcation diagrams of budding yeast cells. (A) Wild-type (this article), (B) wild-type (Chen's 2004 model (15)), (C) *cdh1*Δ ( $k_{ah1p} = k_{ah1pp} = 0$ ), (D) *cki*Δ ( $k_{sip} = k_{sipp} = 0$ ), (E) *cdc20*Δ ( $k_{s20p} = k_{s20pp} = 0$ ), (F) *cdc14*Δ ( $[Cdc14]_{total} = 0$ ). See Fig. 2 for key to diagrams. (A, B, and D) The large-amplitude, stable limit cycles arise from SNIPER bifurcations; (C) they arise from a subcritical Hopf bifurcation followed by a cyclic fold bifurcation. Simulations are consistent with observed phenotypes: *cdh1*Δ and *cki*Δ are viable; *cdc20*Δ and *cdc14*Δ are inviable (blocked in late mitosis), with much higher activity of cyclin B-dependent kinase in *cdc20*Δ than in *cdc14*Δ.

Fig. 6 shows the relationship between limit cycle period and distance from the SNIPER bifurcation. For mass  $< 1.13$ , there is no limit cycle; the stable attractor is the G1 steady state. For mass slightly  $> 1.13$ , the limit cycle period is very long, approaching infinity as mass approaches 1.13 from above. Depending on MDT, the cell cycle trajectory finds a location on the cell-mass axis such that the average cell-cycle-progression time (time spent in G1/S/G2/M) is equal to the mass doubling time. For MDT = 90 min (bottom curve in Fig. 6), the cell is born at mass = 2 and divides at mass = 4, spending its entire lifespan in the oscillatory region, with an average cell-cycle-progression time of 90 min. As MDT lengthens to 120 min (second curve from bottom), the cell cycle trajectory shifts to smaller size, so that the average cell-cycle-progression time can lengthen to 120 min. Still slower growth rates (MDT  $\geq 150$  min) drive the newborn cell into the "sizer" domain, where the Cdk-control system can wait indefinitely at the stable G1 state until the cell grows large enough to surpass the SNIPER bifurcation. Notice that cell-size homeostasis is possible in the "oscillator" domain because of the inverse relationship between oscillator period and cell mass close to a SNIPER bifurcation.

Cell cycles that visit the "sizer" domain (top two curves in Fig. 6) show "strong" size control, i.e., interdivision time is

strongly negatively correlated to birth size, and cell size at the size-controlled transition point (G1 to S in Fig. 6) shows little or no dependence on birth size (1,2). Cell cycles that live wholly in the "oscillator" domain (bottom two curves in Fig. 6) show "weak" size control, i.e., interdivision time is weakly negatively correlated to birth size and there is no clear "critical size" for any cell cycle transition. Nonetheless, such cycles still show balanced growth (interdivision time = mass doubling time) because the cell cycle trajectory settles on a size interval for which the average oscillatory period is identical to the cell's mass doubling time. Balanced growth and division is a consequence of the steep decline in limit cycle period with increasing cell size past the SNIPER bifurcation.

As Fig. 6 demonstrates, for cells in the "oscillator" domain, our model predicts a positive correlation between growth rate and average cell size (faster growing cells are bigger). This correlation is a characteristic and advantageous feature of yeast cells: rich media favor cell growth, poor media favor cell division (50,71). Although it is satisfying to see our model explain this correlation in an "unforced" way, we note that our interpretation of the dependence of cell size on growth rate is predicated on the assumption that one can vary mass doubling time without changing any rate constants in the Cdk-control system (i.e., without changing the location

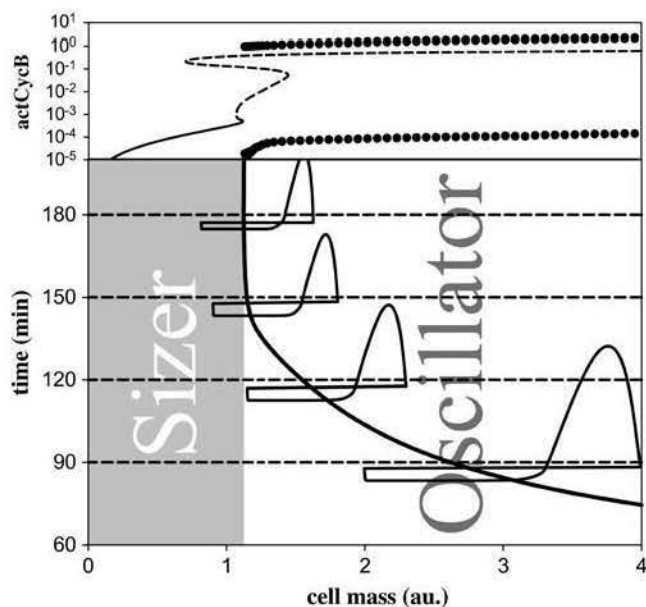


FIGURE 6 Achieving balanced growth at different growth rates. (Upper panel) Bifurcation diagram of the budding yeast network (same as Fig. 5 A). (Lower panel) Period of the oscillatory solutions. Cell cycle trajectories at different MDT (solid curves) are displayed at the corresponding period (dashed lines). Background shading shows the “sizer” and “oscillator” regimes of cell cycle regulation. Slowly growing cells spend part of their cell cycle in a stable G1-arrested state, until they grow large enough to surpass the SNIPER bifurcation and enter S/G2/M; these cells exhibit “strong” size control. Rapidly growing cells are large enough to stay always in the oscillatory regime, maintaining balanced growth and division by finding an average cell-cycle time = MDT. These cells display “weak” size control.

of the bifurcation points in Fig. 6). Unfortunately, this assumption is probably incorrect because changes in growth medium (sugar source, nitrogen source, etc.) likely induce changes in gene expression that move the SNIPER bifurcation points, with poorer growth medium favoring smaller size for completion of the cell cycle (see, e.g., (49,50)). We have yet to sort out all the complications of size regulation in yeast cells. In the meantime, Fig. 6 provides a useful paradigm for understanding “strong” and “weak” size control in eukaryotes.

#### Mutants of G1 phase regulation

In this section we present bifurcation diagrams for a few of the most important and interesting mutants described in great detail by numerical simulations in Chen et al. (15). We start with mutants missing the components that stabilize the G1 phase of the cell cycle: either Cdh1 (an activator of CycB degradation) (Fig. 5 C) or Sic1 (a cyclin B-dependent kinase inhibitor) (Fig. 5 D). In both cases the mutant cells are viable and apparently have a short G1 phase (72–74). On the bifurcation diagrams, however, a stable G1 steady state exists only at very small cell size. In both mutants, the cell cycle trajectory is operating in the “oscillator” domain of

the size-homeostasis diagram, and consequently these mutant cells are expected to exhibit “weak” size control. In these cases, the G1 phase of the cell cycle is a transient state, as described above, and the START transition (G1-to-S) is governed by an oscillator not a sizer. Furthermore, if these mutant cells are grown from spores (i.e., very small size initially), they will execute START at a much smaller size than they do under normal proliferating conditions.

Two-parameter bifurcation diagrams (genetic-physiology planes) for both *SIC1* and *CDH1* are presented in the Supplementary Material (Fig. S3). The two types of mutations have quite a similar effect on cell physiology.

#### Mutants of mitotic exit regulation

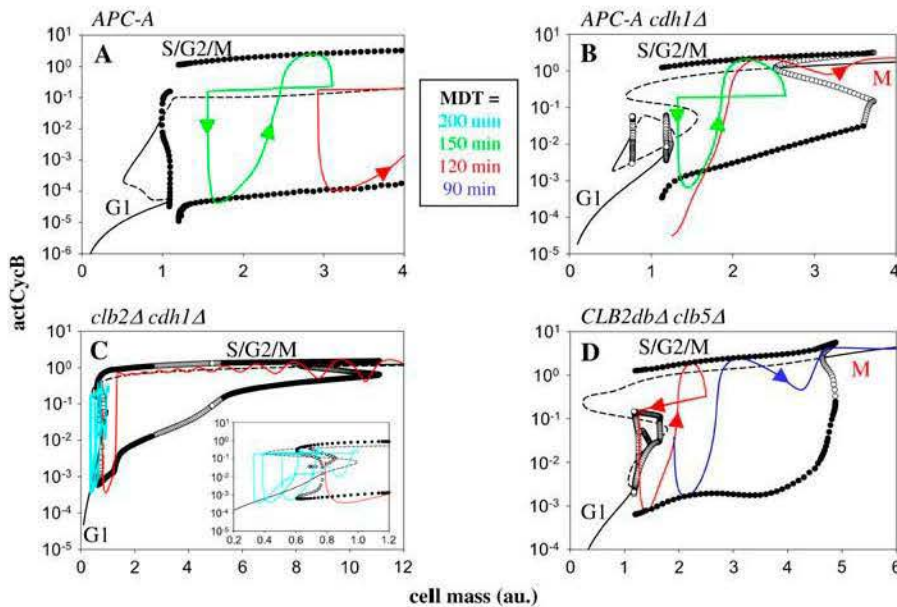
Although both *cdc20<sup>ts</sup>* and *cdc14<sup>ts</sup>* mutants block mitotic exit, *cdc20<sup>ts</sup>* arrests at the metaphase-anaphase transition (75), whereas *cdc14<sup>ts</sup>* arrests in telophase (76,77). Hence, exit from mitosis must be a two-stage process (30), with two different stable-steady states in which the control system can halt. The one-parameter bifurcation diagrams (Fig. 5, E and F) reveal these two stable steady states. For *cdc20<sup>ts</sup>* the steady state has very large CycB activity (~60 au), whereas the *cdc14<sup>ts</sup>* mutant arrests in a state of much lower CycB activity (~2 au). Also, in the second case a damped oscillation is seen on the simulation curve. These effects all derive from the fact that if Cdc20 is inoperable, then cyclin degradation is totally inhibited, whereas if Cdc14 is not working, then Cdc20 can destroy some CycB—not enough for mitotic exit, but enough to create a stable steady state of lower CycB activity (30). The corresponding two-parameter bifurcation diagrams of *cdc20<sup>ts</sup>* and *cdc14<sup>ts</sup>* mutants (Supplementary Material, Fig. S3, C and D) are also qualitatively similar.

#### Lethality that depends on growth rate

To bind effectively to Cdc20, proteins of the core APC need to be phosphorylated (78). If these phosphorylation sites are mutated to nonphosphorylatable alanine residues (the mutant is called APC-A), then Cdc20-mediated degradation of CycB is compromised, although the APC-A cells are still viable. We assume that APC-A has a constant activity that is 10% of the maximum activity of the normally phosphorylated form of APC in conjunction with Cdc20. Furthermore, we assume that APC-A has full activity in conjunction with Cdh1, in accord with the evidence (78). In simulations (Fig. 7 A), APC-A cells are viable and large. Because these mutant cells are delayed in exit from mitosis, the period of the limit cycle oscillations beyond the SNIPER bifurcation is considerably longer than in wild-type cells. Hence, they cycle in the “oscillator” regime even at MDT > 150 min.

Double mutant cells, APC-A *cdh1*Δ, are lethal at fast growth rates but partially viable at slow growth rates (30). Our bifurcation diagram (Fig. 7 B) shows a truncated oscillatory regime ending at a cyclic fold bifurcation at cell





**FIGURE 7** One-parameter bifurcation diagrams of budding yeast mutants defective in cyclin degradation. (A) *APC-A* ([APCP] = 0.1 au, constant value), (B) *APC-A cdh1Δ* ([APCP] = 0.1 au,  $k_{ah1p} = k_{ah1pp} = 0$ ), (C) *clb2Δ cdh1Δ* ( $k_{sbp} = 0.0015 \text{ min}^{-1}$ ,  $k_{sbpp} = 0.015 \text{ min}^{-1}$ ,  $k_{ah1p} = k_{ah1pp} = 0$ ), (D) *CLB2dbΔ clb5Δ* ( $k_{dbsp} = 0.03 \text{ min}^{-1}$ ,  $k_{dbsp} = k_{sap} = k_{sapp} = 0$ ). Notation as in Fig. 2. (A, B, and D) The large-amplitude, stable limit cycles arise from SNIPER bifurcations; (C) they arise from a subcritical Hopf bifurcation followed by a cyclic fold bifurcation (inset). All these mutations compromise one or more of the negative feedback signals that promote exit from mitosis. The latter three show growth rate dependence of viability: slowly growing cells are viable, but rapidly growing cells become stuck in M phase.

mass = 3.6. Simulations show that at MDT = 150 min cells stay within the small oscillatory regime, but faster growing cells (MDT = 120 min) grow out of the oscillatory regime and get stuck in mitosis. Mutations of APC core proteins also show growth rate-dependent viability, e.g., *apc10-22* is viable in galactose (slow growth rate) but inviable in glucose (fast growth rate) (79).

The same dependence of viability on growth conditions was reported for *CLB2dbΔ clb5Δ* mutant cells (CycB stabilized, CycA absent) (30,80), and is illustrated in our bifurcation diagram (Fig. 7 D). In addition to these mutants, which are defective in cyclin degradation, Cross (30) found that the double mutant *clb2Δ cdh1Δ* also shows growth rate-dependent viability. In our model these cells are viable at MDT = 200 min, but lethal at MDT = 120 min (Fig. 7 C).

All of these mutations interfere with the negative feedback loop of CycB degradation. Weak negative feedback creates long-period oscillations that are stable attractors only at relatively small cell mass; at large mass the activity of CycB-dependent kinase is so strong that the mutant cells arrest in mitosis. Fast growing cells cannot find a period of oscillation that balances their MDT, so they overgrow the oscillatory region and get stuck in mitosis. These results suggest that other mutants affecting the negative feedback loop should be reinvestigated to see if viability depends on growth rate (for example, *APC-A sic1Δ* and *cdc20<sup>ts</sup> pds1Δ*).

Cells that show this sensitivity to growth rate are also likely to be sensitive to random noise in the control system. Using a model similar to ours, Battogtokh and Tyson (34) showed that, for control systems operating close to a bifurcation to the stable M-like steady state, cells might get stuck in mitosis after a few cycles if a little noise is added to the system. This effect would show up as partial viability of a clone at intermediate growth rates.

#### Incorporation of the morphogenetic checkpoint

In modeling the budding yeast cell cycle so far, we have assumed that the G2 module of Cdk phosphorylation (module 5 in Fig. 1) plays no role during normal cell proliferation (81), but recently this view was challenged by Kellogg (82). In any event, all agree that the G2 module is necessary for the “morphogenesis checkpoint” in budding yeast, which arrests a cell in G2 if the cell is unable to produce a bud (81). It is a simple job to “turn on” module 5 in our generic version of the budding yeast cell cycle and to reproduce most of the results in Ciliberto et al. (83); see Supplementary Material, Fig. S4.

#### Mammalian cells

Many groups have modeled various aspects of the molecular machinery controlling mammalian cell cycles (22,26,84,85), including us (41). In this article, we insert parameter values from Novak and Tyson (41) into our generic model to simulate a “generic mammalian cell” (Fig. 8). As expected the bifurcation diagram of the mammalian cell (Fig. 8 B) is very similar to the budding yeast cell (there is no G2 module in either model). This yeast-like proliferation is observed in mammalian cells in early development and in malignant transformation, when the cell’s main goal is rapid reproduction.

It has been recently discovered that mouse embryos deleted of all forms of CycD (86), deleted of both forms of CycE (87), or deleted of both Cdk4 and Cdk6 (88) can develop until late stages of embryogenesis and die from causes unrelated to the core cell cycle machinery. Mice lacking Cdk2 are viable (89), and mouse embryo fibroblast from any of these mutants proliferate normally. Our model is expected to reproduce these results. Indeed, simulation of CycE-deleted



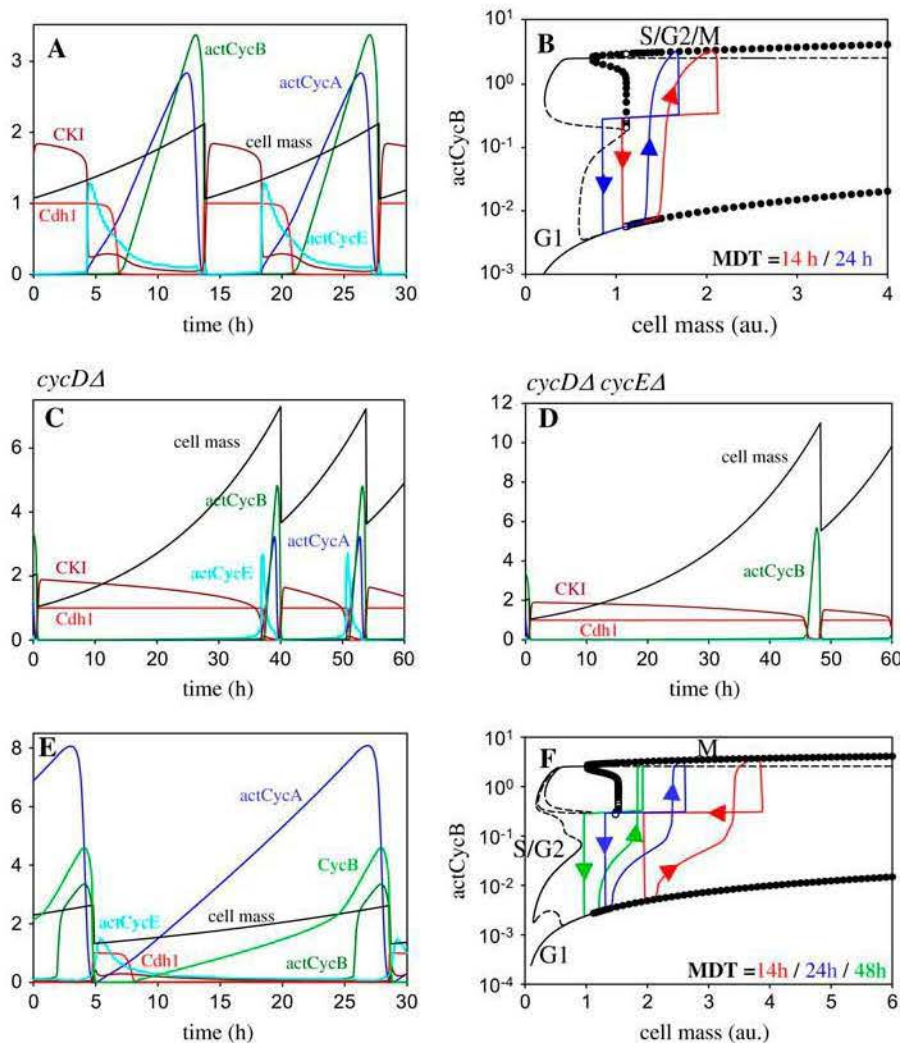


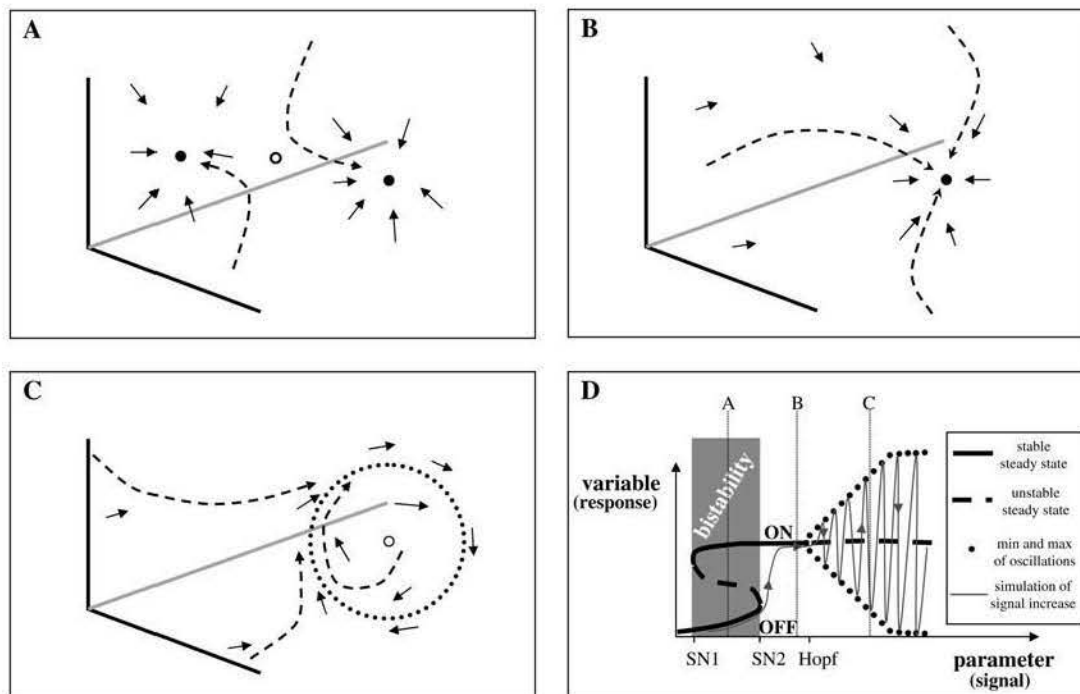
FIGURE 8 Analysis of a mammalian cell cycle model. Numerical simulations: (A) normal cell (without G2 module), (C) *cycD* $\Delta$  ( $CycD^0 = 0$ ), (D) *cycD* $\Delta$  *cycE* $\Delta$  ( $CycD^0 = 0$ ,  $k_{sep} = k_{sepp} = 0$ ), (E) normal cell (with G2 module). One-parameter bifurcation diagrams for normal cell cycles without (B) and with (F) the G2 module.

cells show almost no defect in proliferation with a cell division mass 1.2 times wild-type cells (Supplementary Material, Fig. S5 C). The absence of CycD has a greater effect on the system, creating cycles with a division mass 3.6 times wild-type (Fig. 8 C). If we eliminate both CycD and CycE, we find that cells leave G1 phase at a mass equal to 5 times wild-type division mass (Fig. 8 D), which might be lethal for cells. These results are related to the corresponding experiments in budding yeast, where *cln3*<sup>−</sup> (CycD) and *cln1*<sup>−</sup> *cln2*<sup>−</sup> (CycE) mutants are viable but larger than wild-type (90), whereas the combined mutation is lethal (91).

From Chow et al. (92) we know that, although phosphorylation of Cdk2 (in complexes with CycE or CycA) plays no major role in unperturbed proliferation of HeLa cells, phosphorylation of Cdk1/CycB by Wee1 plays a role in normal cell cycling. These reactions (module 5 in Fig. 1) are easily added to the model, as we did in the previous section on budding yeast. For the parameter values chosen, the bifurcation diagram (Fig. 8 F) exhibits stable G1 and G2 steady states. The cell cycle trajectories in Fig. 8, E and F, are

computed for cells proliferating at MDT = 24 h, that operate in the “oscillator” region of the size homeostasis curve (Fig. 6). More slowly proliferating cells (MDT = 48 h) pause in the stable G1 state until they grow large enough to surpass the SNIPER bifurcation at cell mass  $\sim 1$ . At all growth rates, there is a transient G2 state on the trajectory (the flattened regions of the red and blue curves at  $[actCycB] \sim 0.01\text{--}0.1$ ).

With the G2-regulatory module in place, our model is now set up for serious consideration of the major checkpoint controls in mammalian cells: 1), restriction point control, by which cyclin D and retinoblastoma protein regulate the activity of transcription factor E; 2), the DNA-damage checkpoint in G1, which upregulates the production of CKI; 3), the unreplicated-DNA checkpoint in G2, which activates Wee1 and inhibits Cdc25; and 4), the chromosome misalignment checkpoint in M phase, which silences Cdc20. Building appropriate modules for these checkpoints and wiring them into the generic cell cycle engine will be topics for future publications and will provide a basis for modeling the hallmarks of cancer (93).



**FIGURE 9** Attractors and their bifurcations. (A–C) Examples of vector fields in a three-dimensional state space. Solid arrows, vector field; dashed arrows, simulation results; solid circles, stable steady state; open circles, unstable steady state; dotted circle, stable limit cycle. (D) The transitions (bifurcations) between the vector fields of panels A–C are represented on a one-parameter bifurcation diagram. Solid line, locus of stable steady states; dashed line, locus of unstable steady states, black dots, maximum and minimum values of response variable on a periodic orbit; SN = saddle-node, HB = Hopf bifurcation. The light gray curve indicates a simulation of the response of the control system for a slow increase in signal strength. At SN2, the system jumps from the OFF state to the ON state, and at HB it leaves the steady state and begins to oscillate with increasing amplitude. Within the region of bistability, the control system can persist in either the OFF state or the ON state, depending on how it was prepared (a phenomenon called “hysteresis”).

## DISCUSSION

We propose a protein interaction network for eukaryotic cell cycle regulation that 1), includes most of the important regulatory proteins found in all eukaryotes, and 2), can be parameterized to yield accurate models of a variety of specific organisms (budding yeast, fission yeast, frog eggs, and mammalian cells). The model is built in modular fashion: there are four synthesis-and-degradation modules (“4, 8, 10, 13”), three stoichiometric binding-and-inhibition modules (“6, 9, 12”), three transcription factor modules (“3, 7, 11”), and three modules with multiple activation-and-inhibition steps (“1, 2, 5”). This modularity assists us to craft models for specific organisms (where some modules are more important than others) and to extend models with new modules embodying the signaling pathways that impinge on the underlying cell cycle engine.

To describe the differences in regulatory networks in yeasts, frog eggs, and mammalian cells, we subdivided the generic wiring diagram (Fig. 1) into 13 small modules. From a different point of view (36,37) we might lump some of these modules into larger blocks: bistable switches and negative feedback oscillators. One bistable switch creates a stable G1 state and controls the transition from G1 to S phase. It is a redundant switch, created by interactions between B-type cyclins and

their G1 antagonists: CKIs (stoichiometric inhibitors) and APC/Cdh1 (proteolytic machinery). Either CKI or Cdh1 can be knocked out genetically, and the switch may still be functional to some extent. A second bistable switch creates a stable G2 state and controls the transitions from G2 to M phase. It is also a redundant switch, created by double-negative feedback between Cdk/CycB and Wee1 and positive feedback between Cdk/CycB and Cdc25. A negative feedback loop, set up by the interactions among Cdk/CycB, APC/Cdc20, and Cdc14 phosphatase, controls exit from mitosis. A second negative feedback loop, between CycA and its transcription factor, plays a crucial role in endoreplication. These regulatory loops are responsible for the characteristic bifurcations that (as our analysis shows) control cell cycle progression in normal cells and misprogression in mutant cells.

The many different control loops in the “generic” model can be mixed and matched to create explicit models of specific organisms and mutants. In this sense, there is no “ideal” or “simplest” model of the cell cycle. Each organism has its own idiosyncratic properties of cell growth and division, depending on which modules are in operation, which depends ultimately on the genetic makeup of the organism. Lethal mutations push the organism into a region of parameter space where the control system is no longer viable.

To deepen our understanding of the similarities and differences in cell cycle regulation in different types of cells, we analyzed our models of specific organisms and mutants with bifurcation diagrams. To show how cell growth drives transitions between cell cycle phases (G1/S/G2/M), we employ one-parameter bifurcations diagrams, where stable steady states correspond to available arrest states of the cell cycle (late G1, late G2, metaphase) and saddle-node and SNIPER bifurcation points identify critical cell sizes for leaving an arrest state and proceeding to the next phase of the cell cycle. In this view, cell cycle “checkpoints” (also called “surveillance” mechanisms) (4,5) respond to potential problems in cell cycle progression (DNA damage, delayed replication, spindle defects) by stabilizing an arrest state, i.e., by putting off the bifurcation to much larger size than normal (18,37,40,84,94).

The most important type of bifurcation, we believe, is a “SNIPER” bifurcation, by which a stable steady state (G1 or G2) gives rise to a limit cycle solution that drives the cell into mitosis and then back to G1 phase. At the SNIPER bifurcation, the period of the limit cycle oscillations is initially infinite but drops rapidly as the cell grows larger. SNIPER bifurcations are robust properties of nonlinear control systems with both positive and negative feedback. Not only are they commonly observed in one-parameter bifurcation diagrams of the Cdk network, but they persist over large ranges of parameter variations, as is evident from our two-parameter bifurcation

diagrams. For example, in Figs. 3 B and 4 B, SNIPER bifurcations are observed over the entire range of gene expression for *wee1* and *cdc13* in fission yeast. The same is true for *SIC1* gene expression in budding yeast (Supplementary Material, Fig. S3 B), but not so for *CDC20* and *CDC14* genes (Fig. S3, C and D). In the latter cases, the SNIPER bifurcation is lost for low levels of expression of these essential (“cdc”) genes, and the mutant cells become arrested in late mitotic stages, as observed. Although SNIPER bifurcations are often associated with robust cell cycling in our models, they are not necessary for balanced growth and division, as is evident in our simulation of *cdh1Δ* mutants of budding yeast (Fig. 5 C and Supplementary Material, Fig. S3 A), where the stable oscillations can be traced back to a subcritical Hopf bifurcation.

The SNIPER bifurcation is very effective in achieving a balance between progression through the cell cycle (interdivision time (IDT)) and overall cell growth (mass doubling time (MDT)). Cell size homeostasis means that  $IDT = MDT$ . In Fig. 6 we show that cell size homeostasis is a natural consequence of the eukaryotic cell cycle regulatory system, and that it can be achieved in two dramatically different ways: by a “sizer” mechanism (characteristic of slowly growing cells) and an “oscillator” mechanism (employed by rapidly growing cells). In the sizer mechanism, slowly growing cells are “captured” by a stable steady state, either a G1-like steady state (as in budding yeast) or a G2-like steady state (as in fission yeast).

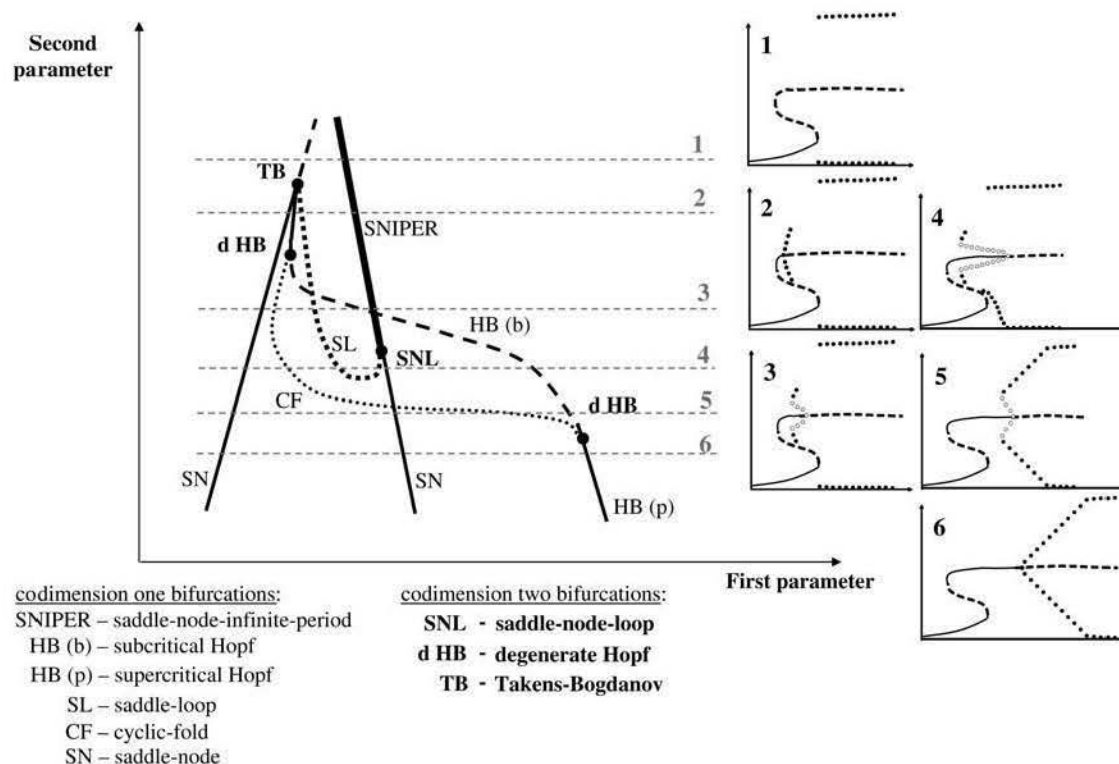


FIGURE 10 An illustrative (hypothetical) two-parameter bifurcation diagram with one-parameter cuts (1–6). See Table 2 for the nomenclature of codimension-one and codimension-two bifurcation points.



To progress further in the cell cycle, these sizer-controlled cells must grow large enough to surpass the critical size at the SNIPER bifurcation. In the oscillator mechanism, rapidly growing cells persist in the limit cycle regime (with cell mass always greater than the critical size at the SNIPER bifurcation), finding a specific combination of average size and average limit-cycle period such that  $IDT = MDT$ . In the oscillator regime, cells are unable to arrest in G1 or G2 phase because they are too large. To arrest, they must undergo one or more divisions, without intervening mass doubling, so that they become small enough to be caught by a stable steady state, or the SNIPER bifurcation point must be shifted to a larger size (by a surveillance mechanism), to arrest the cells in G1 or G2.

One-parameter bifurcations diagrams succinctly capture the dependence of the cell cycle engine (Cdk/CycB activity) on cell growth and division (cell mass changes). By superimposing cell cycle trajectories on the one-parameter bifurcation diagram, we have shown how SNIPER bifurcations orchestrate the balance between cell growth and progression through the chromosome replication cycle. In a two-parameter bifurcation diagram, we suppress the display of Cdk/CycB activity (i.e., the state of the engine) and use the second dimension to display a genetic characteristic of the control system (i.e., the level of expression of a gene, from zero, to normal, to overexpression). On the two-parameter diagram we see how the orchestrating SNIPER bifurcations change in response to mutations, and consequently how the phenotype of the organism (viability/inviability and cell size) depends on its genotype. The two-parameter bifurcation diagram can be used not only to obtain an overview of known phenotypes but also to predict potentially unusual phenotypes of cells with intermediate levels of gene expression.

Our model is freely available to interested users in three forms. From the web site (69) one can download .ode and .set files for use with the free software XPP-AUT. From an .ode file one can easily generate FORTRAN or C++ subroutines, or port the model to Matlab or Mathematica. Secondly, one can download an SBML version of the model from the same web site for use with any software that reads this standard format. Thirdly, we have introduced the model and all the mutant scenarios discussed in this article into JigCell, our problem-solving environment for biological network modeling (95–97). The parameter sets in the JigCell version of budding yeast and fission yeast are slightly different from the parameter sets presented in this article. The revised parameter values give better fits to the phenotypic details of yeast mutants. JigCell is especially suited to this sort of parameter twiddling to optimize the fit of a model to experimental details.

## APPENDIX: A DYNAMICAL PERSPECTIVE ON MOLECULAR CELL BIOLOGY

A molecular regulatory network, such as Fig. 1, is a set of chemical and physical processes taking place within a living cell. The temporal changes driven by these processes can be described, at least in a first approximation, by a set of ordinary differential equations derived according to the standard principles of biophysical chemistry (36). Each differential equation

describes the rate of change of a single time-varying component of the network (gene, protein, or metabolite—the state variables of the network) in terms of fundamental processes like transcription, translation, degradation, phosphorylation, dephosphorylation, binding, and dissociation. The rate of each step is determined by the current values of the state variables and by numerical values assigned to rate constants, binding constants, Michaelis constants, etc. (collectively referred to as parameters).

Given specific values for the parameters and initial conditions (state variables at time = 0), the differential equations determine how the regulatory network will evolve in time. The direction and speed of this change can be represented by a vector field in a multidimensional state space (Fig. 9 A). A numerical simulation moves through state space always tangent to the vector field. Steady states are points in state space where the vector field is zero. If the vector field close to a steady state points back toward the steady state in all directions (Fig. 9 B), then the steady state is (locally) stable; if the vector field points away from the steady state in any direction (near the open circles in Fig. 9, A and C), the steady state is unstable. If the vector field supports a closed loop (Fig. 9 C), then the system oscillates on this periodic orbit, also called a limit cycle. The stability of a limit cycle is defined analogously to steady states. Stable steady states and stable limit cycles are called attractors of the dynamical system. To every attractor is associated a domain of attraction, consisting of all points of state space from which the system will go to that attractor.

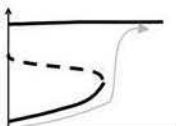
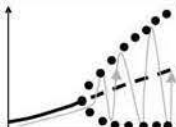
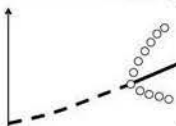
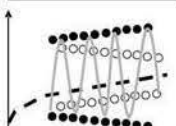
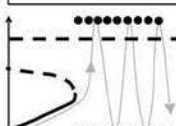
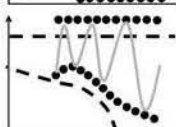
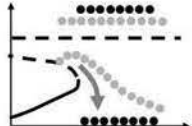

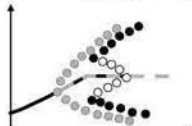
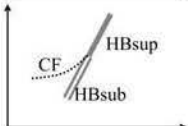

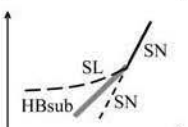
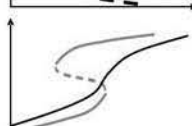
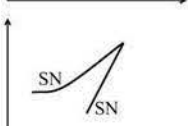
As parameters of the system are changed, the number and stability of steady states and periodic orbits may change, e.g., going from Fig. 9, A to B, or from Fig. 9, B to C. Parameter values where such changes occur are called bifurcation points (98,99). At a bifurcation point, the system can gain or lose a stable attractor, or undergo an exchange of stabilities. In the case of the cell cycle, we associate different cell cycle phases to different attractors of the Cdk-regulatory system, and transitions between cell cycle phases to bifurcations of the dynamical system (37).

To visualize bifurcations graphically, one plots on the ordinate a representative variable of the dynamical system, as an indicator of the system's state, and on the abscissa, a particular parameter whose changes can induce the bifurcation (Fig. 9 D). It is fruitful to think of changes to the parameter as a signal imposed on the control system, and the stable attractors (steady states and oscillations) as the response of the network (100). For the cell cycle control system, the clear choice of dynamic variable is the activity of Cdk1/CycB (the activity of this complex is small in G1, modest in S/G2, and large in M phase). As bifurcation parameter, we choose cell mass because we consider growth to be the primary driving force for progression through the cell cycle. For each fixed value of cell mass, we compute all steady-state and oscillatory solutions (stable and unstable) of the Cdk-regulatory network, and we plot these solutions on a one-parameter bifurcation diagram (Fig. 9 D).

Following standard conventions, we plot steady-state solutions by lines: solid for stable steady states and dashed for unstable. For limit cycles, we plot two loci: one for the maximum and one for the minimum value of Cdk1/CycB activity on the periodic solution, denoting stable limit cycles with solid circles and unstable with open circles. A locus of steady states can fold back on itself at a saddle-node (SN) bifurcation point (where a stable steady state—a node—and an unstable steady state—a saddle—come together and annihilate one another). Between the two SN bifurcation points in Fig. 9 D, the control system is bistable (coexistence of two stable steady states, which we might call OFF and ON). To the left and right of SN2 in Fig. 9 D, the state space looks like Fig. 9, A and B, respectively. A locus of steady-state solutions can also lose stability at a Hopf bifurcation (HB) point, from which there arises a family of small amplitude, stable limit cycle solutions (Fig. 9 D). A Hopf bifurcation converts state space Fig. 9 B into Fig. 9 C. For experimental verification of these dynamical properties of the cell cycle control system in frog eggs, see recent articles by Sha et al. (94) and Pomerening et al. (63,101).

Positive feedback is often associated with bistability of a control system. For example, if X activates Y and Y activates X, then the system may persist in a stable "OFF" state (X low and Y low) or in a stable "ON" state (X high

**TABLE 2** Definitions and examples of codimension-one and -two bifurcations

Codimension-one bifurcations					
Full name	Abbreviation	From/to	To/from	1D example	
Saddle-node	SN	3 steady states	1 steady state		
Supercritical Hopf	HBsup	1 stable steady state	Unstable steady state + small amplitude, stable limit cycle		
Subcritical Hopf	HBsub	1 unstable steady state	Stable steady state + small amplitude, unstable limit cycle		
Cyclic-fold	CF	No oscillatory solutions	1 stable oscillation + 1 unstable oscillation		
Saddle-node infinite-period	SNIPER	3 steady states	Unstable steady state + large amplitude oscillation		
Saddle-loop	SL	Unstable steady state (saddle)	Unstable steady state + large amplitude oscillation		
Codimension-two bifurcations					
Full name	Abbreviation	From/to	To/from	1D example	2D example
Saddle-node loop	SNL	SN + SL	SNIPER		
Degenerate Hopf	dHB	HBsup	HBsub + CF		
Takens-Bogdanov	TB	SN + HB + SL	SN		
CUSP	CUSP	Bistability (2 SN)	Monostability		

and Y high). Similarly, if X inhibits Y and Y inhibits X (double-negative feedback), the system may also persist in either of two stable steady states (X high and Y low, or X low and Y high). Typically, bistability is observed over a range of parameter values ( $k_{SN1} < k < k_{SN2}$ ). Negative feedback (X activates Y, which activates Z, which inhibits X) may lead to sustained oscillations of X, Y, and Z, for appropriate choices of reaction kinetics and rate constants. These oscillations typically arise by a Hopf bifurcation, with a stable steady state for  $k < k_{HB}$  giving way to stable oscillations for  $k > k_{HB}$ .

In Table 2 we provide a catalog of common codimension-one bifurcations (bifurcations that can be located, in principle, by changing a single parameter of the system). From a one-parameter bifurcation diagram, properly interpreted, one can reconstruct the vector field (see lines A, B, and C in Fig. 9D), which is the mathematical equivalent of the molecular wiring diagram. There are only a small number of common codimension-one bifurcations (see Table 2); hence, there are only a few fundamental signal-response relationships from which a cell must accomplish all the complex signal processing it requires. Of special interest to this article is the SNIPER bifurcation, which is a special type of SN bifurcation point: after annihilation of the saddle and node, the remaining steady state is unstable and surrounded by a stable limit cycle of large amplitude. At the SN bifurcation point, the period of the limit cycle is infinite (SNIPER = saddle-node infinite-period). As the bifurcation parameter pulls away from the SNIPER point, the period of the limit cycle decreases precipitously (see, e.g., Fig. 6).

To continue this process of abstraction, we go from a one-parameter bifurcation diagram to a two-parameter bifurcation diagram (Fig. 10). As the two parameters change simultaneously, we follow loci of codimension-one bifurcation points in the two-parameter plane. For example, the one-parameter diagram in Fig. 9D corresponds to a value of the second parameter at level 6 in Fig. 10. As the value of the second parameter increases, we track SN1 and SN2 along fold lines in the two-parameter plane. Between these two fold lines the control system is bistable. We also track the HB point in the two-parameter diagram for increasing values of the second parameter. We find that, at characteristic points in the two-parameter plane, marked by heavy "dots" in Fig. 10, there is a change in some qualitative feature of the codimension-one bifurcations. Because two parameters must be adjusted simultaneously to locate these "dots", they are called codimension-two bifurcation points. In Fig. 10 (and Table 2) we illustrate the three most common codimension-two bifurcations: degenerate Hopf (dHB), saddle-node-loop (SNL), and Takens-Bagdanov (TB). From a two-parameter bifurcation diagram, properly interpreted, one can reconstruct a sequence of one-parameter bifurcation diagrams (see lines 1–6 in Fig. 10), which are the qualitatively different signal-response characteristics of the control system. There are only a small number of generic codimension-two bifurcations; hence, there are limited ways by which one signal-response curve can morph into another. These constraints place subtle restrictions on the genetic basis of cell physiology.

In the one-parameter bifurcation diagram, we choose as the primary bifurcation parameter some physiologically relevant quantity (the "signal") that is inducing a change in behavior (the "response") of the molecular regulatory system. In the two-parameter diagram, we propose to use the second parameter as an indicator of a genetic characteristic of the cell (the level of expression of a particular gene, above and below the wild-type value) with bearing on the signal-response curve. In this format, the two-parameter bifurcation diagram provides a highly condensed summary of the dynamical links from a controlling gene to its physiological outcome (its phenotypes). The two-parameter diagram captures the sequence of dynamically distinct changes that must occur in carrying phenotype of a wild-type cell to the observed phenotypes of deletion mutants (at one extreme) and overexpression mutants (at the other extreme). In between, there may be novel, physiologically distinct phenotypes that could not be anticipated by intuition alone. Examples of this analysis are provided in Figs. 3 and 4, in the Supplementary Material, and on our website.

For alternative explanations of bifurcation diagrams, one may consult the appendix to Borisuk and Tyson (33) or the textbooks by Strogatz (99) or Kaplan and Glass (102).

## SUPPLEMENTARY MATERIAL

An online supplement to this article can be found by visiting BJ Online at <http://www.biophysj.org>.

We thank Jason Zwolak for help with the Supplementary Material and Akos Sveiczzer for useful discussions.

This research was supported by grants from Defense Advanced Research Project Agency (AFRL F30602-02-0572), the James S. McDonnell Foundation (21002050), and the European Commission (COMBIO, LSHG-CT-503568). A.C.N. is a Bolyai fellow of the Hungarian Academy of Sciences.

## REFERENCES

1. Rupes, I. 2002. Checking cell size in yeast. *Trends Genet.* 18:479–485.
2. Sveiczzer, A., B. Novak, and J. M. Mitchison. 1996. The size control of fission yeast revisited. *J. Cell Sci.* 109:2947–2957.
3. Nurse, P. 1994. Ordering S phase and M phase in the cell cycle. *Cell.* 79:547–550.
4. Hartwell, L. H., and T. A. Weinert. 1989. Checkpoints: controls that ensure the order of cell cycle events. *Science.* 246:629–634.
5. Nasmyth, K. 1996. Viewpoint: putting the cell cycle in order. *Science.* 274:1643–1645.
6. Tyson, J. J. 1985. The coordination of cell growth and division—intentional or incidental. *Bioessays.* 2:72–77.
7. Kastan, M. B., and J. Bartek. 2004. Cell-cycle checkpoints and cancer. *Nature.* 432:316–323.
8. Cross, F. R., V. Archambault, M. Miller, and M. Klovstad. 2002. Testing a mathematical model for the yeast cell cycle. *Mol. Biol. Cell.* 13:52–70.
9. Nurse, P. 1992. Eukaryotic cell-cycle control. *Biochem. Soc. Trans.* 20:239–242.
10. Nurse, P. 1990. Universal control mechanism regulating onset of M-phase. *Nature.* 344:503–508.
11. Bray, D. 1995. Protein molecules as computational elements in living cells. *Nature.* 376:307–312.
12. Aguda, B. D. 1999. A quantitative analysis of the kinetics of the G2 DNA damage checkpoint system. *Proc. Natl. Acad. Sci. USA.* 96:11352–11357.
13. Aguda, B. D. 1999. Instabilities in phosphorylation-dephosphorylation cascades and cell cycle checkpoints. *Oncogene.* 18:2846–2851.
14. Chen, K. C., A. Csikasz-Nagy, B. Györfy, J. Val, B. Novak, and J. J. Tyson. 2000. Kinetic analysis of a molecular model of the budding yeast cell cycle. *Mol. Biol. Cell.* 11:369–391.
15. Chen, K. C., L. Calzone, A. Csikasz-Nagy, F. R. Cross, B. Novak, and J. J. Tyson. 2004. Integrative analysis of cell cycle control in budding yeast. *Mol. Biol. Cell.* 15:3841–3862.
16. Goldbeter, A. 1991. A minimal cascade model for the mitotic oscillator involving cyclin and cdc2 kinase. *Proc. Natl. Acad. Sci. USA.* 88:9107–9111.
17. Gonze, D., and A. Goldbeter. 2001. A model for a network of phosphorylation-dephosphorylation cycles displaying the dynamics of dominoes and clocks. *J. Theor. Biol.* 210:167–186.
18. Novak, B., and J. J. Tyson. 1993. Numerical analysis of a comprehensive model of M-phase control in *Xenopus* oocyte extracts and intact embryos. *J. Cell Sci.* 106:1153–1168.
19. Novak, B., and J. J. Tyson. 1995. Quantitative analysis of a molecular model of mitotic control in fission yeast. *J. Theor. Biol.* 173:283–305.
20. Obeyesekere, M. N., J. R. Herbert, and S. O. Zimmerman. 1995. A model of the G1 phase of the cell cycle incorporating cyclinE/cdk2 complex and retinoblastoma protein. *Oncogene.* 11:1199–1205.
21. Obeyesekere, M. N., E. Tecarro, and G. Lozano. 2004. Model predictions of MDM2 mediated cell regulation. *Cell Cycle.* 3:655–661.



22. Qu, Z. L., J. N. Weiss, and W. R. MacLellan. 2003. Regulation of the mammalian cell cycle: a model of the G(1)-to-S transition. *Am. J. Physiol. Cell Physiol.* 284:C349–C364.
23. Qu, Z. L., J. N. Weiss, and W. R. MacLellan. 2004. Coordination of cell growth and cell division: a mathematical modeling study. *J. Cell Sci.* 117:4199–4207.
24. Steuer, R. 2004. Effects of stochasticity in models of the cell cycle: from quantized cycle times to noise-induced oscillations. *J. Theor. Biol.* 228:293–301.
25. Sveiczler, A., A. Csikász-Nagy, B. Györfy, J. J. Tyson, and B. Novak. 2000. Modeling the fission yeast cell cycle: quantized cycle times in *wee1cdc25Δ* mutant cells. *Proc. Natl. Acad. Sci. USA.* 97:7865–7870.
26. Swat, M., A. Kel, and H. Herzel. 2004. Bifurcation analysis of the regulatory modules of the mammalian G(1)/S transition. *Bioinformatics.* 20:1506–1511.
27. Thron, C. D. 1991. Mathematical analysis of a model of the mitotic clock. *Science.* 254:122–123.
28. Thron, C. D. 1997. Bistable biochemical switching and the control of the events of the cell cycle. *Oncogene.* 15:317–325.
29. Tyson, J. J. 1991. Modeling the cell division cycle: *cdc2* and cyclin interactions. *Proc. Natl. Acad. Sci. USA.* 88:7328–7332.
30. Cross, F. R. 2003. Two redundant oscillatory mechanisms in the yeast cell cycle. *Dev. Cell.* 4:741–752.
31. Marlovits, G., C. J. Tyson, B. Novak, and J. J. Tyson. 1998. Modeling M-phase control in *Xenopus* oocyte extracts: the surveillance mechanism for unreplicated DNA. *Biophys. Chem.* 72:169–184.
32. Zwolak, J. W., J. J. Tyson, and L. T. Watson. 2005. Globally optimized parameters for a model of mitotic control in frog egg extracts. *IEE Proc. Syst. Biol.* 152:81–92.
33. Borisuk, M. T., and J. J. Tyson. 1998. Bifurcation analysis of a model of mitotic control in frog eggs. *J. Theor. Biol.* 195:69–85.
34. Battogtokh, D., and J. J. Tyson. 2004. Bifurcation analysis of a model of the budding yeast cell cycle. *Chaos.* 14:653–661.
35. Novak, B., Z. Pataki, A. Ciliberto, and J. J. Tyson. 2001. Mathematical model of the cell division cycle of fission yeast. *Chaos.* 11:277–286.
36. Tyson, J. J., K. Chen, and B. Novak. 2001. Network dynamics and cell physiology. *Nat. Rev. Mol. Cell Biol.* 2:908–916.
37. Tyson, J. J., A. Csikász-Nagy, and B. Novak. 2002. The dynamics of cell cycle regulation. *Bioessays.* 24:1095–1109.
38. Qu, Z. L., W. R. MacLellan, and J. N. Weiss. 2003. Dynamics of the cell cycle: checkpoints, sizers, and timers. *Biophys. J.* 85:3600–3611.
39. Novak, B., and J. J. Tyson. 1997. Modeling the control of DNA replication in fission yeast. *Proc. Natl. Acad. Sci. USA.* 94:9147–9152.
40. Novak, B., A. Csikász-Nagy, B. Györfy, K. Chen, and J. J. Tyson. 1998. Mathematical model of the fission yeast cell cycle with checkpoint controls at the G1/S, G2/M and metaphase/anaphase transitions. *Biophys. Chem.* 72:185–200.
41. Novak, B., and J. J. Tyson. 2004. A model for restriction point control of the mammalian cell cycle. *J. Theor. Biol.* 230:563–579.
42. XPP/XPPAUT. 2005. <http://www.math.pitt.edu/~bard/xpp/xpp.html>. [Online.].
43. Generic Cell Cycle Model. 2006. [http://mpf.biol.vt.edu/research/generic\\_model/main/pp/](http://mpf.biol.vt.edu/research/generic_model/main/pp/). [Online.].
44. Giot, L., J. S. Bader, C. Brouwer, A. Chaudhuri, B. Kuang, Y. Li, Y. L. Hao, C. E. Ooi, B. Godwin, E. Vitols, G. Vijayadmodar, P. Pochart, et al. 2003. A protein interaction map of *Drosophila melanogaster*. *Science.* 302:1727–1736.
45. Kohn, K. W. 1999. Molecular interaction map of the mammalian cell cycle control and DNA repair systems. *Mol. Biol. Cell.* 10:2703–2734.
46. Schwikowski, B., P. Uetz, and S. Fields. 2000. A network of protein-protein interactions in yeast. *Nat. Biotechnol.* 18:1257–1261.
47. Uetz, P., L. Giot, G. Cagney, T. A. Mansfield, R. S. Judson, J. R. Knight, D. Lockshon, V. Narayan, M. Srinivasan, P. Pochart, A. Qureshi-Emili, Y. Li, B. Godwin, et al. 2000. A comprehensive analysis of protein-protein interactions in *Saccharomyces cerevisiae*. *Nature.* 403:623–627.
48. Uetz, P., and M. J. Pankratz. 2004. Protein interaction maps on the fly. *Nat. Biotechnol.* 22:43–44.
49. Fantes, P., and P. Nurse. 1977. Control of cell size at division in fission yeast by a growth-modulated size control over nuclear division. *Exp. Cell Res.* 107:377–386.
50. Johnston, G. C., C. W. Ehrhardt, A. Lorincz, and B. L. A. Carter. 1979. Regulation of cell size in the yeast *Saccharomyces cerevisiae*. *J. Bacteriol.* 137:1–5.
51. Jorgensen, P., and M. Tyers. 2004. How cells coordinate growth and division. *Curr. Biol.* 14:R1014–R1027.
52. Nurse, P. 1975. Genetic control of cell size at cell division in yeast. *Nature.* 256:547–551.
53. Dolznig, H., F. Grebien, T. Sauer, H. Beug, and E. W. Mullner. 2004. Evidence for a size-sensing mechanism in animal cells. *Nat. Cell Biol.* 6:899–905.
54. Killander, D., and A. Zetterberg. 1965. A quantitative cytochemical investigation of the relationship between cell mass and initiation of DNA synthesis in mouse fibroblast in vitro. *Exp. Cell Res.* 40:12–20.
55. Zetterberg, A., and O. Larsson. 1995. Cell cycle progression and cell growth in mammalian cells: kinetic aspects of transition events. In *Cell cycle Control*. C. Hutchison and D. M. Glover, editors. Oxford University Press, Oxford, UK. 206–227.
56. Baserga, R. 1984. Growth in size and cell DNA replication. *Exp. Cell Res.* 151:1–4.
57. Conlon, I., and M. Raff. 2003. Differences in the way a mammalian cell and yeast cells coordinate cell growth and cell-cycle progression. *J. Biol.* 2:7.
58. Murray, A. W., and M. W. Kirschner. 1989. Cyclin synthesis drives the early embryonic cell cycle. *Nature.* 339:275–280.
59. Solomon, M. J., M. Glotzer, T. H. Lee, M. Philippe, and M. W. Kirschner. 1990. Cyclin activation of p34<sup>cdc2</sup>. *Cell.* 63:1013–1024.
60. Futcher, B. 1996. Cyclins and the wiring of the yeast cell cycle. *Yeast.* 12:1635–1646.
61. Yang, L., Z. Han, W. Robb MacLellan, J. N. Weiss, and Z. Qu. 2006. Linking cell division to cell growth in a spatiotemporal model of the cell cycle. *J. Theor. Biol.* In press.
62. Moreno, S., and P. Nurse. 1994. Regulation of progression through the G1 phase of the cell cycle by the *rum1*<sup>+</sup> gene. *Nature.* 367:236–242.
63. Pomeroy, J. R., S. Y. Kim, and J. E. Ferrell Jr. 2005. Systems-level dissection of the cell-cycle oscillator: bypassing positive feedback produces damped oscillations. *Cell.* 122:565–578.
64. Ayte, J., C. Schweitzer, P. Zarov, P. Nurse, and J. A. DeCaprio. 2001. Feedback regulation of the MBF transcription factor by cyclin Cig2. *Nat. Cell Biol.* 3:1043–1050.
65. Benito, J., C. Martin-Castellanos, and S. Moreno. 1998. Regulation of the G1 phase of the cell cycle by periodic stabilization and degradation of the p25<sup>rum1</sup> CDK inhibitor. *EMBO J.* 17:482–497.
66. Hayles, J., D. Fisher, A. Woollard, and P. Nurse. 1994. Temporal order of S phase and mitosis in fission yeast is determined by the state of the p34<sup>cdc2</sup>-mitotic B cyclin complex. *Cell.* 78:813–822.
67. Parisi, T., A. R. Beck, N. Rougier, T. McNeil, L. Lucian, Z. Werb, and B. Amati. 2003. Cyclins E1 and E2 are required for endoreplication in placental trophoblast giant cells. *EMBO J.* 22:4794–4803.
68. Nurse, P., P. Thuriaux, and K. Nasmyth. 1976. Genetic control of the cell division cycle in the fission yeast *Schizosaccharomyces pombe*. *Mol. Gen. Genet.* 146:167–178.
69. Computational Cell Biology at Virginia Tech. 2005. <http://mpf.biol.vt.edu/>. [Online.].
70. Tyson, J. J. 1983. Unstable activator models for size control of the cell cycle. *J. Theor. Biol.* 104:617–631.
71. Tyers, M. 2004. Cell cycle goes global. *Curr. Opin. Cell Biol.* 16:602–613.

72. Schwob, E., T. Böhm, M. D. Mendenhall, and K. Nasmyth. 1994. The B-type cyclin kinase inhibitor p40<sup>gic1</sup> controls the G1 to S transition in *S. cerevisiae*. *Cell*. 79:233–244.
73. Visintin, R., S. Prinz, and A. Amon. 1997. *CDC20* and *CDH1*: a family of substrate-specific activators of APC-dependent proteolysis. *Science*. 278:460–463.
74. Zachariae, W., M. Schwab, K. Nasmyth, and W. Seufert. 1998. Control of cyclin ubiquitination by CDK-regulated binding of Hct1 to the anaphase promoting complex. *Science*. 282:1721–1724.
75. Sethi, N., M. C. Monteagudo, D. Koshland, E. Hogan, and D. J. Burke. 1991. The *CDC20* gene product of *Saccharomyces cerevisiae*, a beta-transducin homolog, is required for a subset of microtubule-dependent cellular processes. *Mol. Cell. Biol.* 11:5592–5602.
76. Fitzpatrick, P. J., J. H. Toyn, J. B. Millar, and L. H. Johnston. 1998. DNA replication is completed in *Saccharomyces cerevisiae* cells that lack functional Cdc14, a dual-specificity protein phosphatase. *Mol. Gen. Genet.* 258:437–441.
77. Visintin, R., K. Craig, E. S. Hwang, S. Prinz, M. Tyers, and A. Amon. 1998. The phosphatase Cdc14 triggers mitotic exit by reversal of Cdk-dependent phosphorylation. *Mol. Cell*. 2:709–718.
78. Rudner, A., and A. Murray. 2000. Phosphorylation by Cdc28 activates the Cdc20-dependent activity of the anaphase promoting complex. *J. Cell Biol.* 149:1377–1390.
79. Imiger, S., M. Baumer, and G. H. Braus. 2000. Glucose and Ras activity influence the ubiquitin ligases APC/C and SCF in *Saccharomyces cerevisiae*. *Genetics*. 154:1509–1521.
80. Wasch, R., and F. Cross. 2002. APC-dependent proteolysis of the mitotic cyclin Clb2 is essential for mitotic exit. *Nature*. 418:556–562.
81. Lew, D. J. 2003. The morphogenesis checkpoint: how yeast cells watch their figures. *Curr. Opin. Cell Biol.* 15:648–653.
82. Kellogg, D. R. 2003. Wee1-dependent mechanisms required for coordination of cell growth and cell division. *J. Cell Sci.* 116:4883–4890.
83. Ciliberto, A., B. Novak, and J. J. Tyson. 2003. Mathematical model of the morphogenesis checkpoint in budding yeast. *J. Cell Biol.* 163:1243–1254.
84. Aguda, B. D., and Y. Tang. 1999. The kinetic origins of the restriction point in the mammalian cell cycle. *Cell Prolif.* 32:321–335.
85. Obeyesekere, M. N., E. S. Knudsen, J. Y. Wang, and S. O. Zimmerman. 1997. A mathematical model of the regulation of the G1 phase of Rb+/+ and Rb-/- mouse embryonic fibroblasts and an osteosarcoma cell line. *Cell Prolif.* 30:171–194.
86. Kozar, K., M. A. Ciemerych, V. I. Rebel, H. Shigematsu, A. Zagozdou, E. Sicinska, Y. Geng, Q. Y. Yu, S. Bhattacharya, R. T. Bronson, K. Akashi, and P. Sicinski. 2004. Mouse development and cell proliferation in the absence of D-cyclins. *Cell*. 118:477–491.
87. Geng, Y., Q. Y. Yu, E. Sicinska, M. Das, J. E. Schneider, S. Bhattacharya, W. M. Rideout, R. T. Bronson, H. Gardner, and P. Sicinski. 2003. Cyclin E ablation in the mouse. *Cell*. 114:431–443.
88. Malumbres, M., R. Sotillo, D. Santamaria, J. Galan, A. Cerezo, S. Ortega, P. Dubus, and M. Barbacid. 2004. Mammalian cells cycle without the D-type cyclin-dependent kinases Cdk4 and Cdk6. *Cell*. 118:493–504.
89. Ortega, S., I. Prieto, J. Odajima, A. Martin, P. Dubus, R. Sotillo, J. L. Barbero, M. Malumbres, and M. Barbacid. 2003. Cyclin-dependent kinase 2 is essential for meiosis but not for mitotic cell division in mice. *Nat. Genet.* 35:25–31.
90. Dirick, L., T. Böhm, and K. Nasmyth. 1995. Roles and regulation of Cln/Cdc28 kinases at the start of the cell cycle of *Saccharomyces cerevisiae*. *EMBO J.* 14:4803–4813.
91. Richardson, H. E., C. Wittenberg, F. Cross, and S. I. Reed. 1989. An essential G1 function for cyclin-like proteins in yeast. *Cell*. 59:1127–1133.
92. Chow, J. P. H., W. Y. Siu, H. T. B. Ho, K. H. T. Ma, C. C. Ho, and R. Y. C. Poon. 2003. Differential contribution of inhibitory phosphorylation of CDC2 and CDK2 for unperturbed cell cycle control and DNA integrity checkpoints. *J. Biol. Chem.* 278:40815–40828.
93. Hanahan, D., and R. A. Weinberg. 2000. The hallmarks of cancer. *Cell*. 100:57–70.
94. Sha, W., J. Moore, K. Chen, A. D. Lassaletta, C.-S. Yi, J. J. Tyson, and J. C. Sible. 2003. Hysteresis drives cell-cycle transitions in *Xenopus laevis* egg extracts. *Proc. Natl. Acad. Sci. USA*. 100:975–980.
95. Allen, N. A., L. Calzone, K. C. Chen, A. Ciliberto, N. Ramakrishnan, C. A. Shaffer, J. C. Sible, J. J. Tyson, M. T. Vass, L. T. Watson, and J. W. Zwolak. 2003. Modeling regulatory networks at Virginia Tech. *OMICS*. 7:285–299.
96. Vass, M., N. Allen, C. A. Shaffer, N. Ramakrishnan, L. T. Watson, and J. J. Tyson. 2004. The JigCell model builder and run manager. *Bioinformatics*. 20:3680–3681.
97. JigCell Project. 2005. <http://jigcell.biol.vt.edu/>. [Online].
98. Kuznetsov, Y. A. 1995. Elements of Applied Bifurcation Theory. Springer Verlag, New York.
99. Strogatz, S. H. 1994. Nonlinear Dynamics and Chaos. Addison-Wesley, Reading, MA.
100. Tyson, J. J., K. C. Chen, and B. Novak. 2003. Sniffers, buzzers, toggles, and blinkers: dynamics of regulatory and signaling pathways in the cell. *Curr. Opin. Cell Biol.* 15:221–231.
101. Pomeroy, J. R., E. D. Sontag, and J. E. Ferrell Jr. 2003. Building a cell cycle oscillator: hysteresis and bistability in the activation of Cdc2. *Nat. Cell Biol.* 5:346–351.
102. Kaplan, D., and L. Glass. 1995. Understanding Nonlinear Dynamics, Chapter 5. Springer-Verlag, New York.